Risk imposed on terpen due to liquefaction caused by induced earthquakes

A thesis presented to
the Faculty of Civil Engineering and Geosciences
Delft University of Technology

In partial fulfillment
of the requirements for the bachelor's degree of
Applied Earth Sciences

Under the supervision of
Dr. ir. D.J.M. Ngan-Tillard
&
Dr. ir. W. Broere

by
Salima Oumejjoud
4590317

8-11-2019

Acknowledgements

I would like to express my gratitude for my first supervisor, Dr. ir. Ngan-Tillard, for her patience, advice and good support. Furthermore, I want to thank her for her time and attention. I would also like to say thank you to my second supervisor Dr. ir. Broere for his guidance and feedback.

Preface

In total 326 terpen in the Netherlands are classified as national monuments. A large portion of the terpen are located in the province Groningen. Groningen is often in the news, because of the earthquakes that took place, which were caused by the gas-extraction activities. The earthquakes caused damage to infrastructure and they can also be a threat to the stability of the terpen. Since the earthquakes can lead to soil liquefaction. The goal of this report is to investigate the risk of liquefaction to the terpen due to induced earthquakes. Furthermore, fine sands was the most liquefiable soil type. The Naaldwijk and Eem formations have the highest liquefaction potential based on their soil compositions, densities and age. The Naaldwijk formation is the most prone to liquefaction since it is located more shallow in the underground. Afterwards, cone penetration test data was used to evaluate the soil classes, soil unit weights and soil behaviour indexes. The soil behaviour index values were used to asses the liquefaction potential. In the end, none of the three chosen terpen were liquefiable. Moreover, 2D and 3D visualizations were made in order to better understand the heights and slopes of the terpen.

Content

1. Introduction

The Dutch word for the Netherlands is ‘Nederland’, it contains the word ‘neder’, which means low (Encyclo, n.d.). A reference to the Netherlands being partially below the sea level. About one third is situated below the NAP, as can be seen in figure 1.1. NAP stands for Normaal Amsterdams Peil and it is equal to the average sea level (Rijkswaterstaat, 2019). Nowadays dikes protect the country. Back in the day, before the year 1000 dikes did not exist (Bosschaart & Driessen, 1989). Hence, flooding was a frequent issue the habitants had to deal with. As a solution to the flooding the Dutch started to make terpen for protection, see figure 1.2. Terp is the Dutch word for an inhabited mound. Throughout this report the word terp shall be used. Terpen are protected, because they are archaeologically and culturally valued (Doesburg & Stöver, 2018). They can be found in the provinces Noord-Holland, Friesland and Groningen. The condition of the terpen that are located in Groningen could be threatened by earthquakes. These earthquakes are caused by gas extraction projects. The earthquakes are of low magnitudes and take place in the shallow subsurface causing damage to the ground surface. Among others, the strong ground shaking can lead to soil liquefaction under certain conditions. The goal of this report is to determine whether the Groningse terpen are at risk of soil liquefaction.

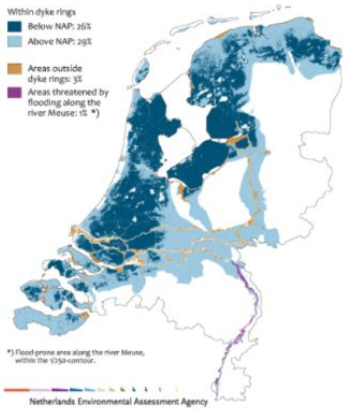

Figure 1.1 Netherlands below NAP (PBL Netherlands Environmental Assesment Agency, n.d.)

Figure 1.2 Terp inhabitants bringing their cattle into safety (Image from terpen exposition in Westerkwartier, in the church of Niehove, n.d.)

First the geographic location and history of terpen are discussed. Second, the gas extraction from the Groningen gas field are described and its effects are presented. Then the geological history is explained in which different formations were formed and deposited. Afterwards the soil liquefaction phenomenon is explained with its influencing factors. Furthermore, cone penetration tests (CPTs) are used to asses the liquefaction potential. The CPT data is used to classify soil layers and to determine the soil behaviour index of each layer. The soil types are assessed with two classification systems, namely the Robertson CPT soil classification chart

and one from a Dutch geotechnical report by ATAR Geotechniek. The soil behaviour index value determines whether there is a risk of liquefaction. Afterwards, the depth stress reduction coefficient (r_d) and magnitude scaling factor (MSF) are explained. These are empirical factors that aid in understanding the soil response to ground shaking. New formulas for the r_d and MSF have been proposed for Groningen to take into account the specificity of the local earthquakes: shallow induced earthquakes of low magnitudes. Then the applied research starts, where three terpen are evaluated on their liquefaction potential. First their selection is discussed as well as some background information. Moreover, the previously explained theory is applied to CPT data in order to asses the liquefaction potential of the three terpen. Furthermore, 2D models of the terpen are shown that were made with AHN2 data in AHN Viewer. Also, 3D models of the three terpen are shown that were made with the use of the QGIS program. These show the geometry of the terpen, which can influence the liquefaction potential. Lastly, a conclusion is drawn from three considered cases and recommendations are made.

2. Literature study

2.1 Geographic location of Dutch terpen

Terpen is the Frisian name for these man-made hills, in Groningen these are called wierden. Furthermore, there are two types of terpen, namely house terpen and village terpen (Doesburg & Stöver, 2018), these can easily be distinguished by their size. Overall, more village than house terpen were built, see figure 2.1.1.

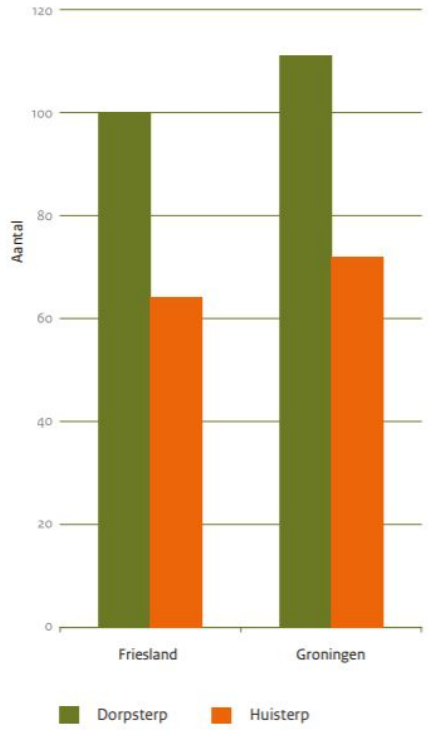

Figure 2.1.1 Amount of village and house terpen in Friesland and Groningen (Doesburg & Stöver, 2018)

Furthermore, terpen can be found in the Northern part of the Netherlands in three provinces, namely Noord-Holland, Friesland and Groningen, see figures 2.1.2 and 2.1.3. The abbreviation AMK stands for ‘Archeologische Monumenten Kaart’, these are areas with archaeological value in the broad sense (bodemrichtlijn, 2019). The term ‘Rijks’ stands for national monument. The main difference between AMK and Rijks is that the national monuments are protected. It should be noted that about a quarter of all the Dutch terpen are classified as Dutch national monuments (Doesburg & Stöver, 2018).

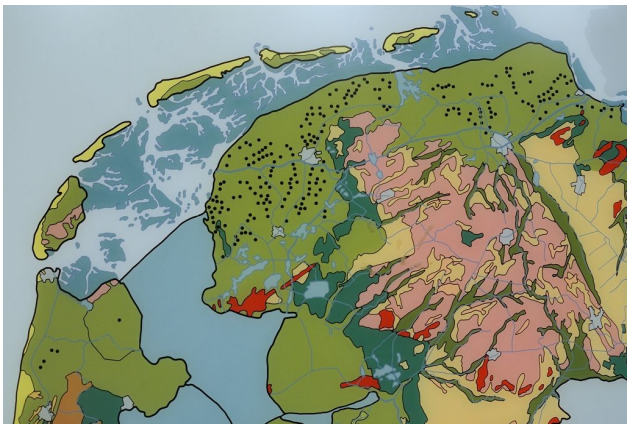

Figure 2.1.2 All Dutch terpen; black dots represent terpen (Picture of map in Museon, n.d.)

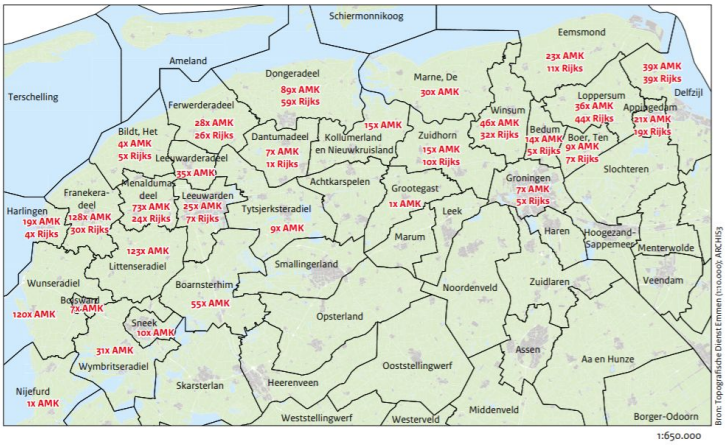

Figure 2.1.3 Geographic location of protected terpen; ‘AMK’ indicates archaeological valued areas and ‘Rijks’ denotes national monuments (Doesburg & Stöver, 2018)

2.2 History of the terpen

In 700 BC the first long term residents of the Northern provinces of the Netherlands inhabited the lands and took refuge onto the terpen during high tides (Schroor, 1998). Dikes were made around the year 1000 (Bosschaart & Driessen, 1989). The terpen were often made of fruitful soils. These soils were valued and therefore excavated after the construction of the dikes for financial reasons, see figure 2.2.1. The excavations caused damage to the terpen (Arjaans, 1990).

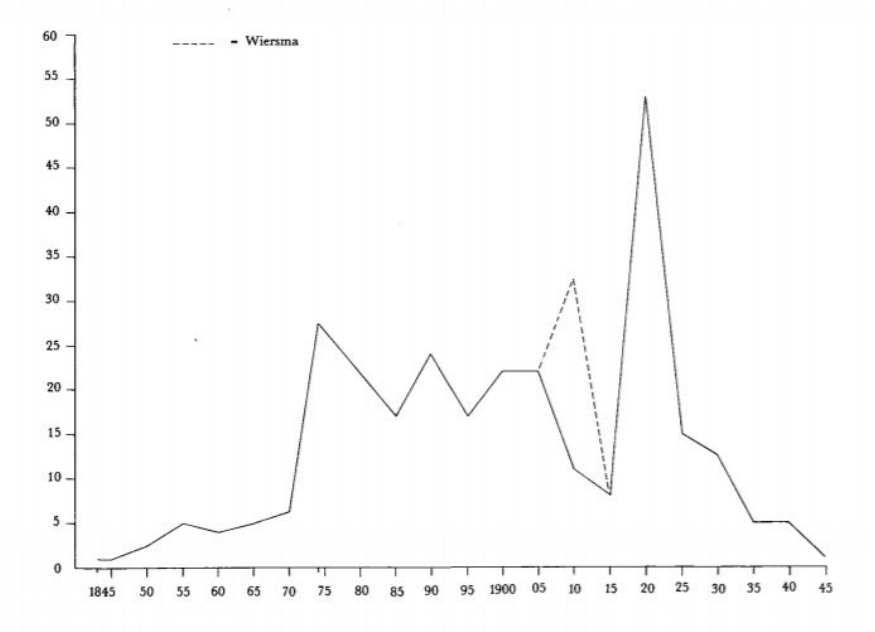

Figure 2.2.1 Amount of Frisian terpen excavated for financial reasons (Arjaans, 1990)

Figure 2.2.2 shows the excavation of the Ferwerd terp.

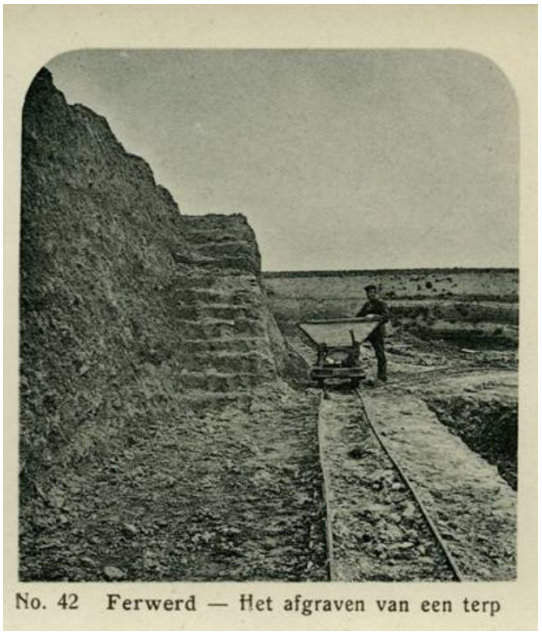

Figure 2.2.2 Excavation of Ferwerd terp (Herwig, 1911)

Excavation of the highest terp of the Netherlands, Hegebeintum started in the year 1900 (Leeuwarder courant, 1900), see figure 2.2.3.


Hoogste Terp
IN FRIESLAND
is geopend te Hogebeintum. Eerste kwaliteit, 50 cent per ton.
Terpbaas P. REITSMA.

Figure 2.2.3 Hegebeintum terp soil for sale (Leeuwarder courant, 1900)

A timeline of all the mentioned events is given in figure 2.2.4.

Figure 2.2.4 Timeline of history of the terpen; Note that the first event happened in 700 BC

Other reasons for terp excavation would be for ground leveling or for the construction industry (Doesburg & Stöver, 2018). In 1943 the Dutch government put a halt on the disturbance of terpen. After the second world war 'de Rijksdienst voor het Oudheidkundig Bodemonderzoek' (ROB) was assigned to make a list of all the valuable terrains from a heritage perspective and to protect and maintain these. In 1964 the first terpen became national monuments. Figure 2.2.5 shows that most village terpen in Groningen and Friesland are nowadays grass fields or meadows. The same goes for the majority of the smaller house terpen (Doesburg & Stöver, 2018).

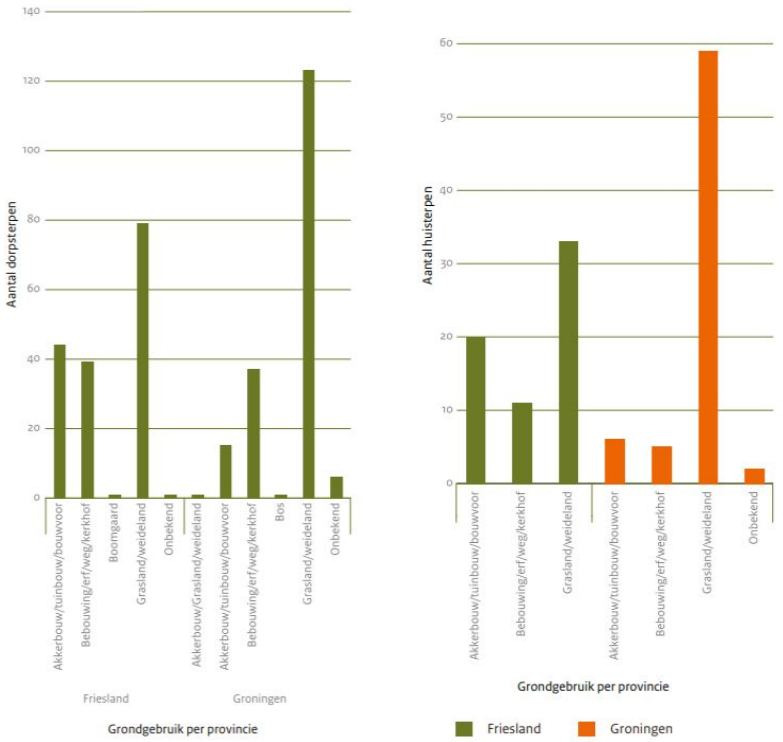

Figure 2.2.5 Land usage village and house terpen in Friesland and Groningen (Doesburg & Stöver, 2018)

2.3 Valuable terpen

Nowadays, 326 of all terpen are a part of the Dutch natural heritage, these are located in the provinces of Friesland and Groningen (Doesburg & Stöver, 2018). Terpen are treasured for their cultural value and archaeological value. Firstly, terpen have cultural value, because they symbolize the fight against the water of the people from that time. Furthermore, these artificial hills are clearly visible in the landscape of the marine clay coastal grounds as a reminder (Doesburg & Stöver, 2018). Secondly, their archaeological value can be easily explained. Since people lived on these terpen, their remnants can be found on these terpen. Figure 2.3.1 shows a highly appreciated artefact from 600 AD. It is a cloak pin that was found in Wijnaldum, Friesland (Historiek, 2015). Even terpen that have been disturbed deserve an archaeological field work, because the bottom of the terp can contain interesting findings, which explains why disturbed terpen are protected by the government (Doesburg & Stöver, 2018).

Figure 2.3.1 Cloak pin found in Wijnaldum (Frisian museum, n.d.)

Terpen are interesting and challenging to investigate, because of their high degree of heterogeneity in terms of soil composition, this can clearly be seen in figures 2.3.2 and 2.3.3 that show core samples of the Frisian terp Hegebeintum. Remains were found such as bones, shreds and coins in the borehole cores. Also soil features indicative of house floors and ditches were identified. Moreover, Hegebeintum is with almost 9 metres above NAP, the highest terp of the Netherlands and Germany (Terp Hegebeintum, n.d.).

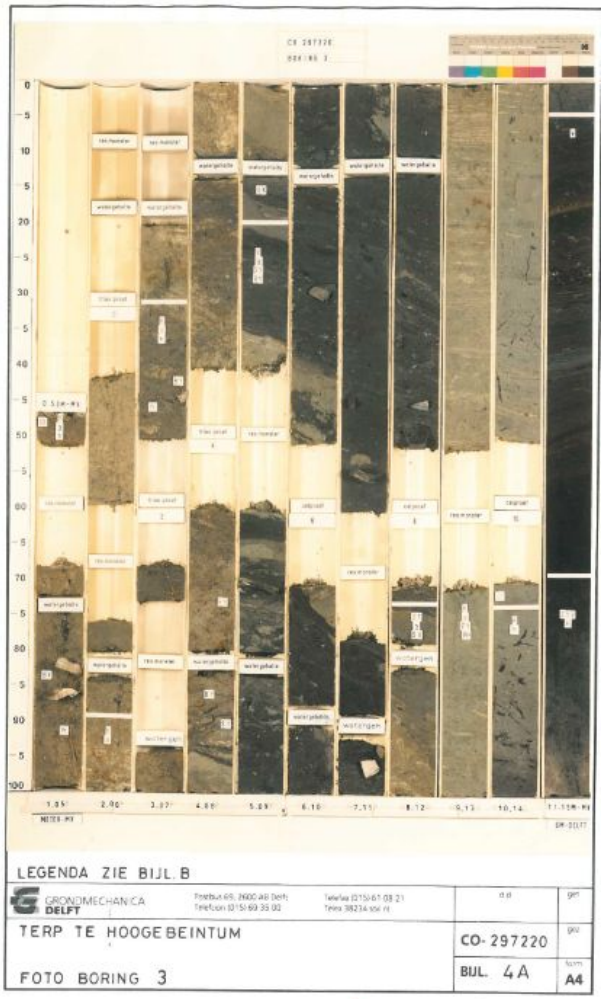

Figure 2.3.2 Borehole logs of Hegebeintum terp (Nicolay et al, 2019)

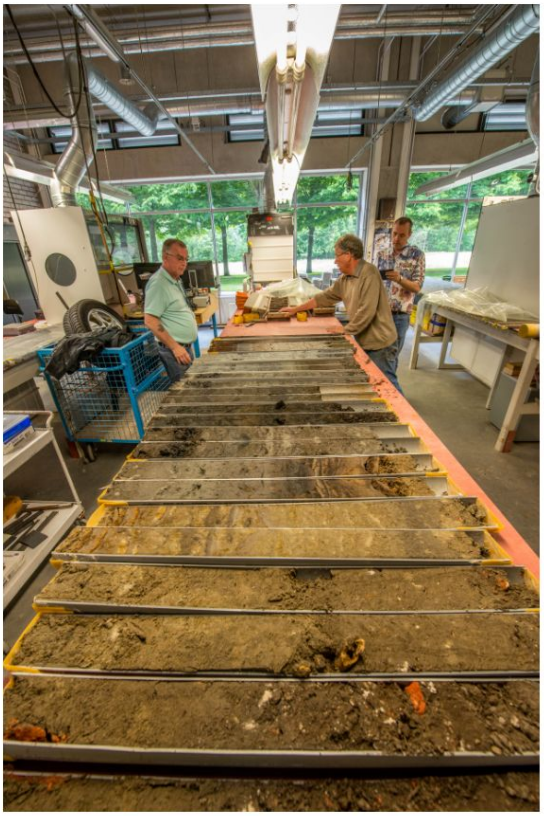

Figure 2.3.3 Borehole samples of Hegebeintum terp (Nicolay et al, 2019)

Another location with archaeological value is Jelsum, a village in the province Leeuwarden. Jelsum was occupied from the Roman times to the Middle ages. In 2010 an archaeological fieldwork took place of Jelsum led by Dr. Johan Nicolay, who is specialized in archeology concerning terpen. Figure 2.3.4 shows the excavation of the trenches and their high variability in soil composition.

Figure 2.3.4 Excavation of Jelsum terp (Ngan-Tillard, n.d.)

2.4 Gas extraction in Groningen

Terpen are located in the Northern part of the Netherlands. In this part of the country gas exploitation occurs. The gas extraction activities have been causing earthquakes, these are also known as induced earthquakes. The strongest earthquakes due to gas exploitation occured in the province Groningen (Mulder & Perey, 2018). The gas field that lies under Groningen was found in 1959 and after 4 years the production started (Whaley, 2009). This is also the largest gas field of the Netherlands (KNMI, n.d.) and the 10th largest in the world (Whaley, 2009), see figure 2.4.1.

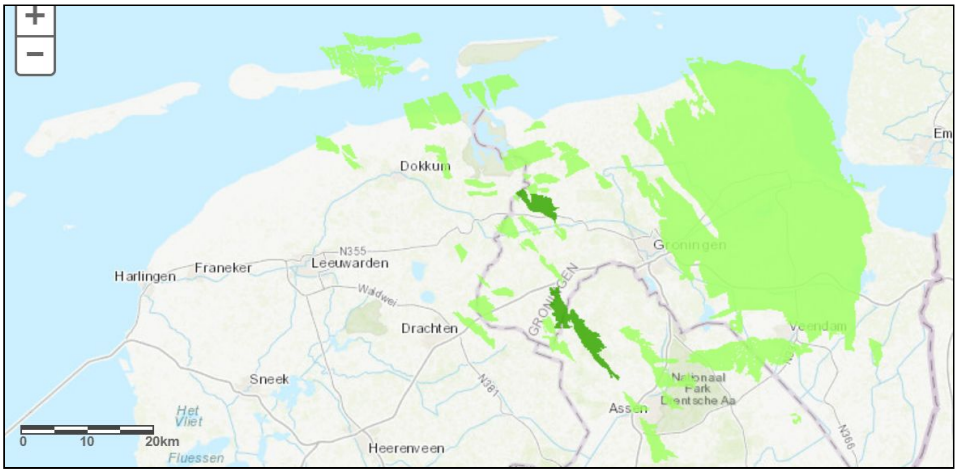

Figure 2.4.1 Groningen gas field, dark green is gas storage, green is gas field (NAM, n.d.)

The Groningen gas field has been of great economic value to the Netherlands. The use of gas has also been good for environmental reasons. Of all the fossil fuels gas has the lowest carbon dioxide emissions. Since gas became a replacement for other fossil fuels, it helped clean the air of Europe (Whaley, 2009). However, in 2012 the downside of the gas exploitation became clear. In August of 2012 an induced earthquake took place near Huizinge with a magnitude of 3.6 on the scale of Richter. The operator of the field, the Nederlandse Aardolie Maatschappij received over 1,000 damage reports in the week following the event (Mulder & Perey, 2018). Afterwards, more earthquakes have taken place with increasing magnitudes, see figure 2.4.2 (NAM, n.d.). All causing the Groningen inhabitants to become angry and frustrated. A great deal of damage was done to their houses, neighbourhoods and villages (Mulder & Perey, 2018). Early 2018 more than 85,000 damage claims have been filed (NCG, 2017). Many Groningen inhabitants are dissatisfied and want the gas operations to stop, to prevent more earthquakes from happening (Mulder & Perey, 2018).

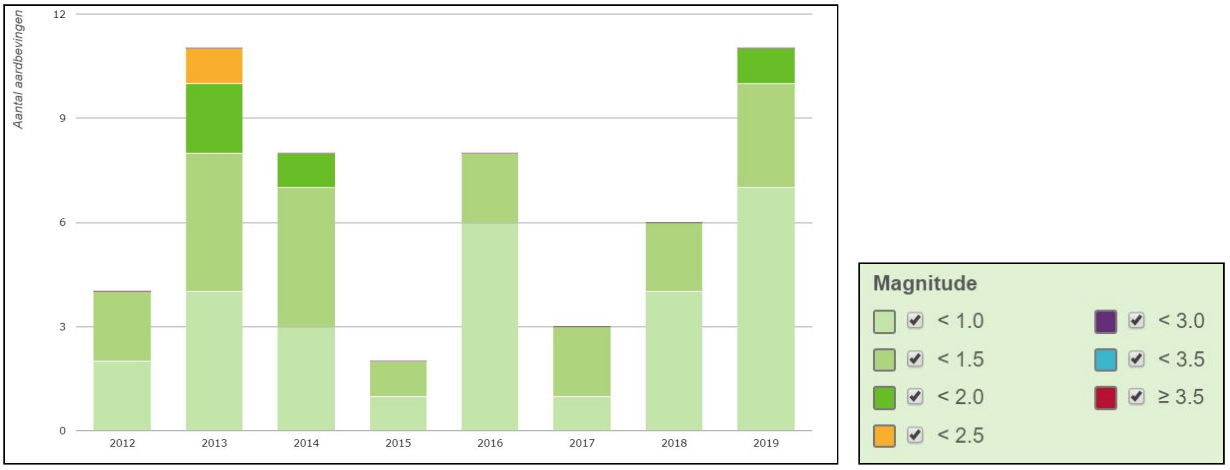

Figure 2.4.2 Earthquakes from 2012 to 2019 of Groningen with legend of magnitudes (NAM, n.d.)

The gas is being retrieved from a porous sandstone reservoir with a surface of 900 km^2 large and a thickness of 100 metres. The reservoir is located about 3 kilometres under the ground (Vlek, 2019). The sand particles in the sandstone are under high pressure. This pressure decreases when gas is extracted from the sandstone. The lower pressure cannot support the weight on top of the sandstone, which results in soil subsidence. In case the above layers undergo compression in a non uniform way, an earthquake follows (Mulder & Perey, 2018). Naturally, greater subsidence will lead to an earthquake with a higher magnitude (KNMI, n.d.). Despite their small magnitude, the earthquakes induced by gas extraction in Groningen have caused damage due to their limited depths.

The KNMI have produced a seismic hazard map, showing the peak ground acceleration (PGA) values of Groningen, see figure 2.4.3 (KNMI, 2017). The induced waves of an earthquake travel through the ground and exert certain forces. These forces are proportionate to the ground velocity, because of Newton's 2nd Law. Furthermore, the PGA depends on the magnitude of the earthquake and the soil type (KNMI, n.d.). It is important to know the PGA since this shows the parts of land that have a higher risk when an earthquake happens, so that preventative plans can be put in action. Another advantage is that it aids in civil engineering. Since higher risk zones should be constructed with stronger foundations.

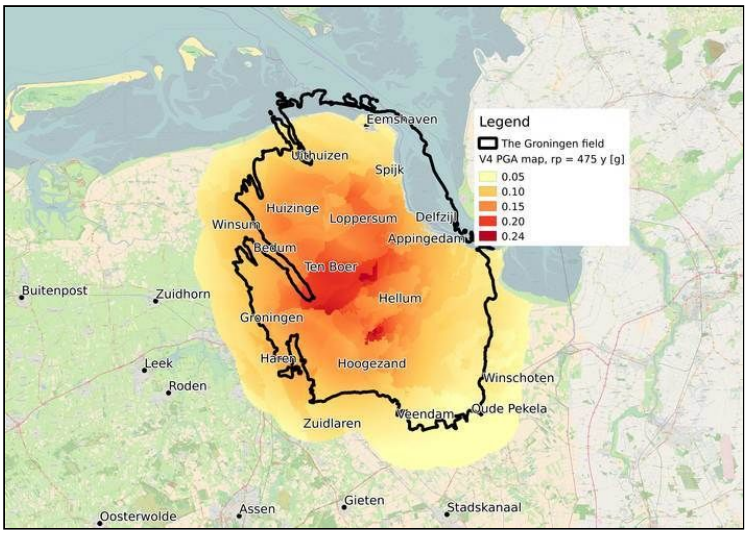

Figure 2.4.3 PGA over the Groningen gas field (KNMI, n.d.)

2.5 Soil liquefaction

A possible consequence of the earthquakes that are happening in Groningen is liquefaction. Liquefaction is a phenomenon that occurs when saturated loosely packed sediments loses their strength due to strong earth shaking (USGS, n.d.). Loosely packed particles are held together by their friction with water filled pore spaces. During the ground shaking the space between particles increases, causing the soil to behave like a liquid. Fine grained type of soils are most likely to liquefaction, such as sandy soils (Encyclopedia Britannica, n.d.). Hence knowing the soil composition is of great importance. Moreover, soil liquefaction mainly occurs to the shallow subsurface. The majority of most recent liquefaction cases do not take place deeper than 20 metres (Boulanger & Idriss, 2014).

The chance on liquefaction can be controlled by sedimentary characteristics and the depositional environment. These include the grain sizes, percentage of fines and sphericity. Secondary processes can also play a role, such as cementation, soil formation, overconsolidation and ageing (Kuivert et al, 2017).

Density of the sediment
One of the conditions for liquefaction is that the soil is loosely packed. The lower the density, the more likely sediments shall undergo liquefaction (USGS, n.d.).

Overconsolidation
After the soil has been subjected to very high stresses and unloaded, the soil rebounds and gains back some of the volume it lost. This process is called overconsolidation (Rajapakse, 2016). A way to measure the overconsolidation is with the OCR. OCR stands for over-consolidation ratio and is equal to the past effective vertical stress over the present effective vertical stress. If the OCR is 1, the sediment is normally consolidated and if the OCR is larger than 1 it is overconsolidated. An increase in the OCR leads to an decrease in the liquefaction potential (Nagase et al, 2000).

Cementation
The process of cementation lowers the liquefaction potential. Since during cementation pores get filled and the density increases (Wayne Clough et al, 1989). Moreover, cementation is expected to be correlated with the deposition age. The older the deposition, the more cementation has taken place (Deltares, 2016), which would lower the liquefaction potential.

Grain size distribution
In figure 2.5.1 the liquefiable soils based on grain size can be seen. The fine grained sands with a low amount of fines are most likely to liquefy (Tsuchida, 1970).

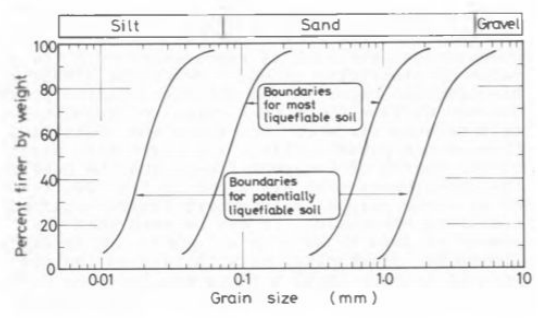

Figure 2.5.1 Liquefiable soils based on grain size (Tsuchida, 1970)

Sphericity

The shape of a particle can impact the likelihood for liquefaction. Though recent research of the Northern Netherlands made clear that the majority of 97% of the sand layers is moderately rounded. The remaining 2% is rounded and the 1% is angular (Bosch et al, 2014). So the shape of particles is not an important factor.

Saturation content

A rise in the sea level can lead to a higher groundwater table. Leading to an increase in the saturation of the soil nearby coastal zones (Nuttle & Portnoy, 1992). Another way sediments become saturated is due to heavy rainfall. Moreover, drainage conditions are important, because they influence the saturation content. The saturation content is important to know, because a high saturation content is a condition for soil liquefaction.

Age and depositional environment

According to research older depositions are less likely to liquefy than younger depositions (Youd and Perkins, 1978). This also depends on the environment of the deposition, see table 2.5.1 (Gillins, 2012). The depositional environments that are present in the shallow underground of Groningen are estuarine, dunes, alluvial fan, glacial till, lacustrine and river channels. Overall, only glacial till shows a low likelihood for liquefaction, all others are moderate to high (Deltares, 2016).

Table 2.5.1 Relation of age and depositional environment to liquefaction (Gillins, 2012)

Type of Deposit (1)	General Distribution of Cohesionless sediments in deposits (2)	Likelihood that Cohesionless Sediments, When Saturated, Would be Susceptible to Liquefaction (by Age of Deposit)			
		<500 yr (3)	Holocene (4)	Pleistocene (5)	Pre-Pleistocene (6)
(a) Continental Deposits					
River Channel	Locally Variable	Very High	High	Low	Very Low
Floodplain	Locally Variable	High	Moderate	Low	Very Low
Alluvial Fan and Plain	Widespread	Moderate	Low	Low	Very Low
MarineTerraces/ Plains	Widespread	-----	Low	Very Low	Very Low
Delta and Fan-delta	Widespread	High	Moderate	Low	Very Low
Lacustrine and Playa	Variable	High	Moderate	Low	Very Low
Colluvium	Variable	High	Moderate	Low	Very Low
Talus	Widespread	Low	Low	Very Low	Very Low
Dunes	Widespread	High	Moderate	Low	Very Low
Loess	Variable	High	High	High	Unknown
Glacial Till	Variable	Low	Low	Very Low	Very Low
Tuft	Rare	Low	Low	Very Low	Very Low
Tephra	Widespread	High	High	?	?
Residual Soils	Rare	Low	Low	Very Low	Very Low
Sebkha	Locally Variable	High	Moderate	Low	Very Low
(b) Coastal Zone					
Delta	Widespread	Very High	High	Low	Very Low
Esturine	Locally Variable	High	Moderate	Low	Very Low
Beach					
High Wave Energy	Widespread	Moderate	Low	Very Low	Very Low
Low Wave Energy	Widespread	High	Moderate	Low	Very Low
Lagoonal	Locally Variable	High	Moderate	Low	Very Low
Fore Shore	Locally Variable	High	Moderate	Low	Very Low
(c) Artificial					
Uncompacted Fill	Variable	Very High	-----	-----	-----
Compacted Fill	Variable	Low	-----	-----	-----

Geometry of the terp

The geometry of a terp has an effect on its stability, since the slopes and heights influence the effective and total stresses, these stresses have an impact on the liquefaction potential. Furthermore, landslide liquefaction can be a consequence of instability. The landslide would cause ground shaking and the liquefiable soil would then undergo liquefaction (van Asch et al, 2006). Moreover, material on a terp with sharp slopes is more likely to slide down, especially after a storm or heavy rainfall.

2.6 Geological history of the Groningen Gas Field region

Figure 2.6.1 shows a cross section that goes up to 500 metres below the subsurface. The cross section starts west in the island Terschelling, passes Groningen and ends near the border with Germany in Nieuwe Schans (Meijles, 2015). Now the history of the deposition of the most important formations shall be discussed. Note that the following overview of the time periods will be very schematic.

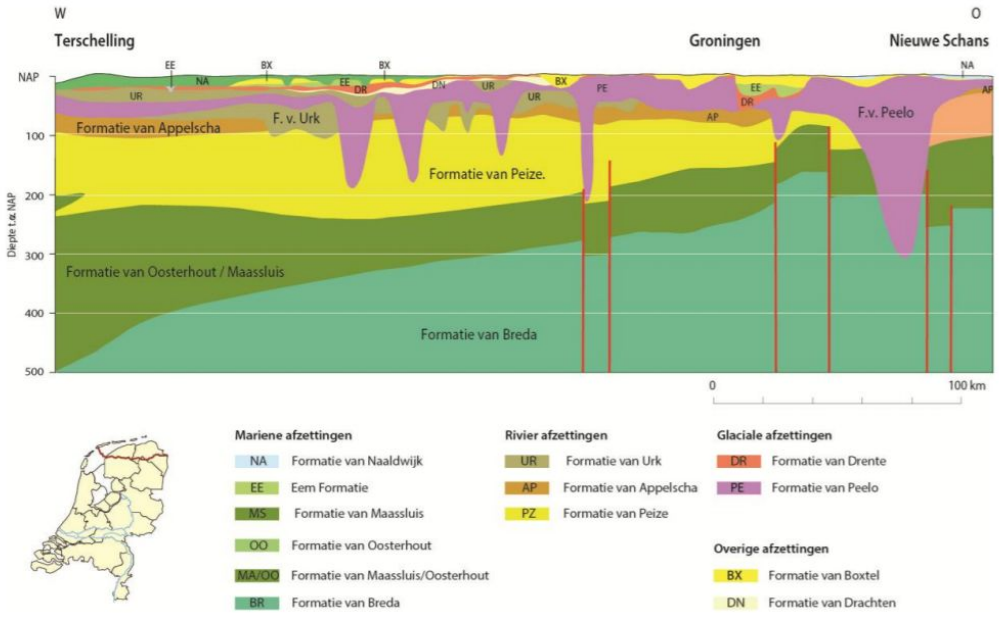

Figure 2.6.1 Cross section from Terschelling to Nieuwe Schans (Meijles, 2015)

The last three ice ages, including their interglacial periods, have shaped the geology of the Northern part of the Netherlands (Meijles, 2015). In between the ice ages there were warm periods. The climate changed frequently from very cold to warm weathers.

Elsterien

The first ice age that covered the North of Netherlands with ice is called the Elsterien (Mulder et al, 2003). All depositions of this ice age is known as the formation of Peelo. Since the soil had to bear the weight of the ice sheet, it is very likely that overconsolidation took place, which decreases the liquefaction potential (Korff et al, 2016). Furthermore, from figure 2.5.1 the formation of Peelo looks the most striking, due to its shape and change in thickness. The thickness of this deposition varies from 20 to 300 metres, due to trenches also known as tunnel valleys (Gans, 2007). These have been interpreted to have formed during meltwater pulses and after their formation they were filled with fluvioglacial sediments.

Another factor that makes the formation more susceptible to liquefaction is its age, the formation is relatively the oldest (Korff et al, 2016), making it less prone to liquefaction. The soil composition consists of sand and clay. The sand from this formation has a high

variability from very fine to very coarse and are mainly well sorted (Korff et al, 2016). Figure 2.6.2 shows the depth and thickness of the Peelo formation.

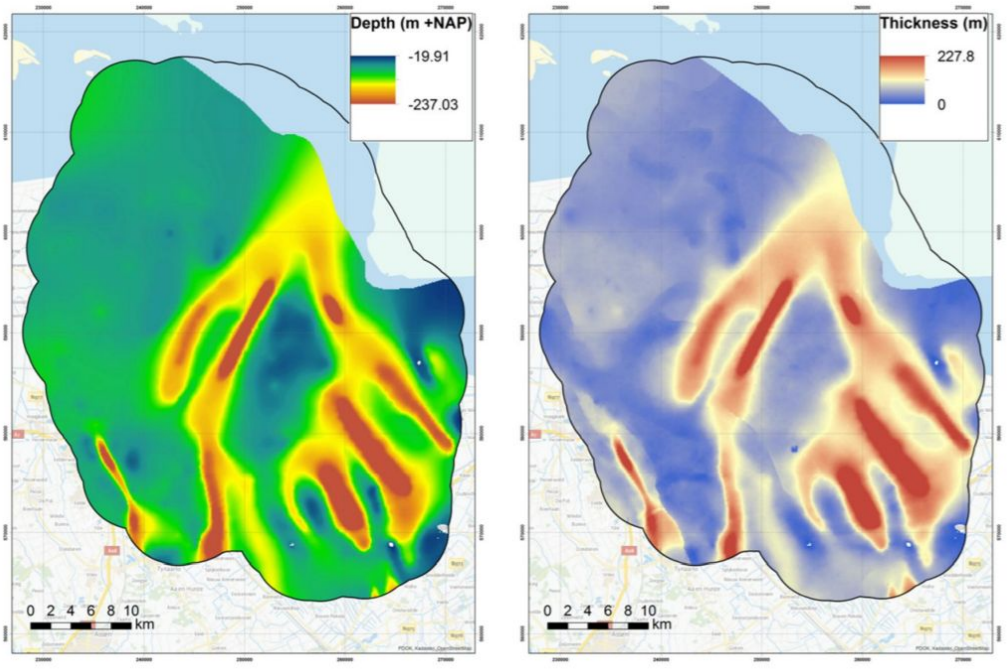

Figure 2.6.2 Depth and thickness of Peelo formation, GeoTOP 3D subsurface model (Maljers et al., 2016)

Holsteinien

After the Elsterien the Holsteinien followed, which was a time period in which the ice melted (Mulder et al, 2003). The depositions from this time period are somewhat unknown. Although there were some marine deposits and mudflat sediment deposits found in Groningen (Mulder et al, 2003).

Saalien

Next the Saalien followed, also known as a complex ice age, due to the frequent transformation from cold to warm periods. The push moraines from this period left a mark in the landscape of today. The main deposit was glacial till. However in some places the soft glacial till was eroded away (Berendsen, 2008). Another type of sediment that was deposited was medium coarse sand. These were left behind by the meltwater streams. The two depositions are known as the formation of Drente (Berendsen, 1998). The sediments have been deposited in a fluvioglacial setting (Korff et al, 2016). Most likely there was no ice sheet loading in this period. Hence, no overconsolidation to take into account, which raises the liquefaction potential. Furthermore, the Drente formation is young, which increases the liquefaction potential (Korff et al, 2016). Figure 2.6.3 shows the depth of the base of the formation and its thickness.

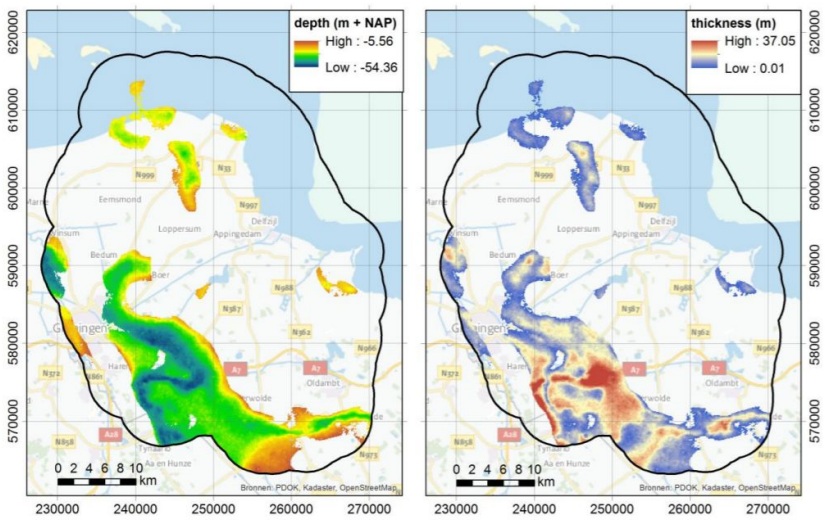

Figure 4.6 Depth of the base (left) and total thickness (right) of the Drente model unit in the GeoTOP 3D subsurface model (Maljers et al., 2016)

Figure 2.6.3 Depth of base and thickness of Drente formation, GeoTOP 3D subsurface model (Maljers et al, 2016)

Eemian

Afterwards the Eemian interglacial period followed. Once again the ice melted in this warmer period. The tides had a large effect on the marine deposition that was formed. The deposition consists of coarse sand that transitions into fine sand and eventually clay (Berendsen, 2008). The main two depositions are from tidal channels and tidal flats. The channels were filled with sand layers that are interrupted by organic clay layers and the sand size is very fine to medium. The tidal flat deposits were deposited in layers of sand and clay. The sand is very fine with some silt and clay (Korff et al, 2016). Furthermore figure 2.6.4 shows where the Eem formation was deposited and its thickness and depth.

The following ice age did not produce an ice sheet. Thus, the sediments of the Eem period have not been overconsolidated, increasing the chance for liquefaction. Moreover, the deposition is similar to the Naaldwijk Formation, but the Eem formation is older (Korff et al, 2016).

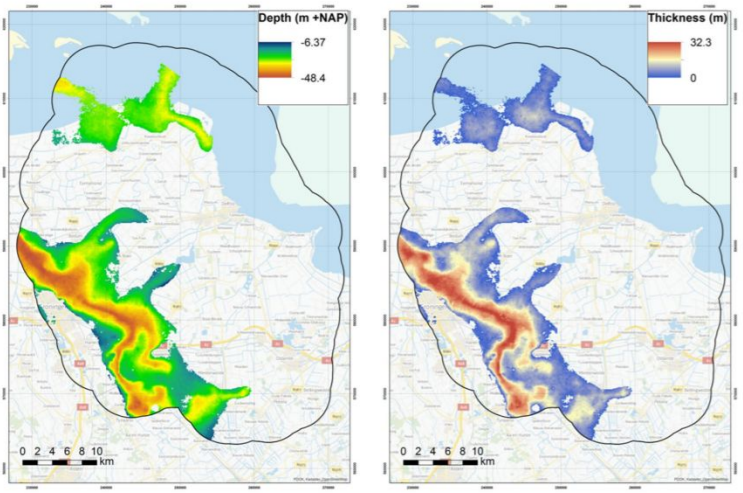

Figure 2.6.4 Depth of base and thickness of Eem formation, GeoTOP 3D subsurface model (Maljers et al, 2016)

Weichselian

Then the last glacial time period took place, named the Weichselian. This is the only time period in which the ice did not reach the Netherlands. Nevertheless it was still a cold environment. All the depositions of this period come back in the Boxtel formation, the soil composition is complex, containing moderately fine to coarse sand. The moderately fine to coarse sand was deposited by the streams. The moderately fine sand is known as 'dekzanden' (translates to cover sands). Within this period there was a very dry and cold period in which there was very little vegetation, also called the polar desert. In that time, the sand got transported by the wind and was deposited elsewhere (Berendsen, 2008), also known as aeolian deposits (Lancaster, 2009). Moreover, the thickness and depth of the Boxtel formation can be seen in figure 2.6.5.

Since there was not ice sheet deposited upon the Boxtel formation, no overconsolidation has taken place, which increases the chance of liquefaction. Moreover, the permafrost lead to cryoturbation which changed the soil composition (Korff et al, 2016). Cryoturbation can cause older lower situated layers to become a part of the younger layers. Thus, making it more difficult to interpret the data properly (Kleber et al, 2013). Overall the Boxtel formation is made up of young sands that includes fine sand, which makes it prone to liquefaction.

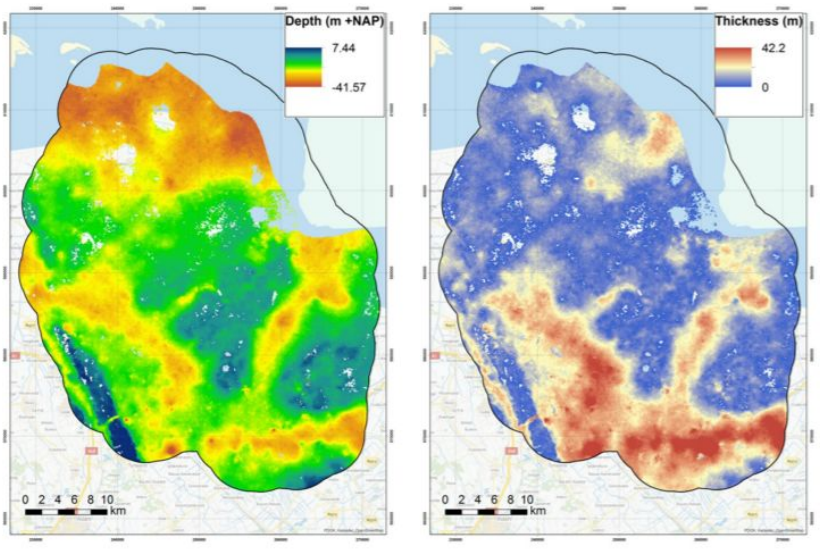

Figure 2.6.5 Depth of base and thickness of Boxtel formation, GeoTOP 3D subsurface model (Maljers et al, 2016)

Holocene

Finally the Holocene followed, which is the current time period. The Holocene is a warm period, with a fast rising water table due to the melting of the ice caps. Since the sea level is rising it leads to the rising of the groundwater table in coastal areas. Leading to the formation of swamps in between the land and sea where plants that have become detritus turn into peat. However, peat also grows on elevated grounds. Mainly due to the glacial till and clay that prevents the drainage of water. These peat depositions are called the formation of Nieuwkoop. Later on, some of the previously deposited peat got eroded away (Vos et al, 2011).

On top of the Nieuwkoop formation, the Naaldwijk formation is deposited in the same time period. The Naaldwijk formation is a relatively young sand deposition. No cementation has occurred, making it more prone to liquefaction. It has also not been affected by an ice age. Thus, the layer has not been loaded by a heavy ice sheet, which would lead to overconsolidation. Hence, a decrease in liquefaction potential. Figure 2.6.6 shows the thickness of the Naaldwijk formation as well as its depth (Korff et al, 2016). Further on, the sea level kept rising, creating more peat. Though erosion also made the peat go away. Salt marshes and mounds were shaped that changed the positioning of trenches and plains, causing a high variability in soil type in coastal regions of Groningen. Afterwards sand and clay sediments were transported and deposited in the coastal plains (Vos et al, 2011). Overall, the sands that the formation contains are tidal channel and tidal flat depositions. The tidal channel deposits are made up of fine to medium sand and the tidal flat of fine sand, clay and loam. The tidal channel deposit is composed of approximately 90% sand and the tidal flat of 60% sand (Korff et al, 2016).

In 500 BC there was an area of salt marshes situated in the northern part of the Groningen gas field of which the first people made it their home. The people were likely attracted due to the fruitful grounds and the decrease in the frequency of floodings (Delvigne, 2008). Soon after, people built their own terpen. Eventually, the coastal deposition stopped when the dikes were placed (Vos et al, 2011).

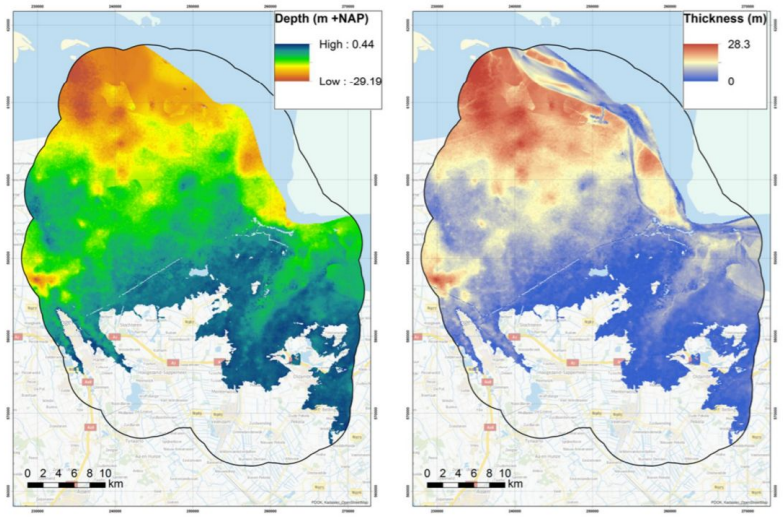

Figure 2.6.6 Depth of base and thickness of Naaldwijk formation, GeoTOP 3D subsurface model (Maljers et al, 2016)

Appendix A1 gives an overview of all the formations in another form, it shows the soil composition and the location of the formations. Moreover, table 2.6.1 shows the factors that influence the liquefaction potential of the different formations.

Table 2.6.1 Liquefaction sensitivity of sandy formations; neutral o, lower -, higher + (Kruiver et al, 2017; Youd & Perkins, 1978; Korff et al, 2017)

		Sensitivity					
Geological unit	Sediment characteristics	Fine sand	Low fines content	Depositional environment	Age	Glacial loading	Associated GeoTOP model units (abbreviations)
Naaldwijk Formation	Abundant fine sand, channels usually clean sand, flats usually silty and commonly bedded with clay/loam lenses.	++	o	++	+	No	NA, NAWA, NAWO
Boxtel Formation	Abundant fine sand, usually clean sand (especially Wierden Member)	++	+	+/−	+	No	BXWI, BXSI2, BX
Eem Formation	Abundant fine sands, cleaner channels but siltier and bedded flats.	+	+	+	+	No	EE
Drente Formation, Schaarsbergen Member	Generally clean and medium coarse sand.	−	+	−	−	No	DR
Urk Formation, Tynje Member	Varying composition with fine to coarse sand, occasionally very silty and bedded with clay/loam beds.	+	+	+	−	Yes	URTY
Peelo Formation	Mostly fine slightly silty sand, partly very coarse clean sand at greater depths.	+	+	−	−	Yes	PE

2.7 Sand formations in the Groningen Gas Field region

The formations that are mainly made up of sand are the Naaldwijk, Boxtel, Eem, Drente, Urk and Peelo formations (Bosch et al., 2014). Relative young sandy depositions that have not undergone glacial loading can be expected to be the most vulnerable to liquefaction, under the assumption that overconsolidation has not taken place (Kruiver et al, 2017).

Sand densities

Figure 2.7.1 gives a clear overview of the sand densities for each formation. The Naaldwijk and Eem formations contain the most loosely packed sands and also the least dense sands. The Naaldwijk and Eem formation consist of 31% and 38% loose sands and the other formations 5-17%. Hence, the Naaldwijk and Eem formations are most prone to liquefaction based on sand densities.

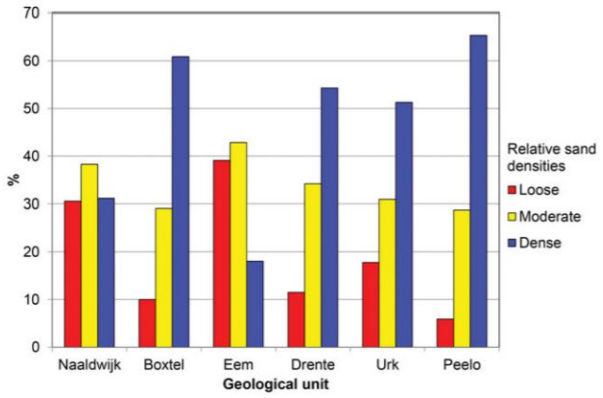

Figure 2.7.1 Sand densities of sand in six formations (Kruiver et al., 2017)

Moreover, younger sands are more prone to liquefaction, because they are located in the shallow subsurface. The Eem formation is positioned lower in the surface, making it less prone to liquefaction (Kruiver et al., 2017).

Geographical location

Furthermore, it is striking that the Naaldwijk sands are mostly deposited in the northern part of the study area, whereas the Pleistocene sands are mainly deposited in the south, see figure 2.7.2. In terms of soil composition, the Naaldwijk formation contains more silt and more clay and silt beddings than the Eem formation (Bosch et al., 2014).

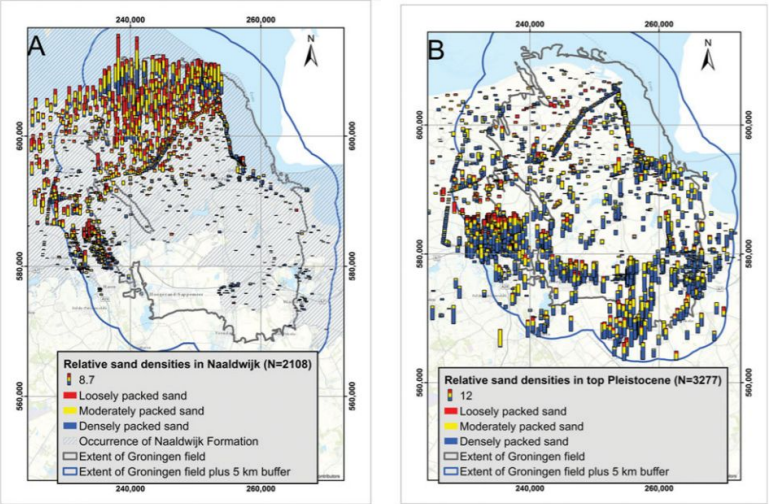

Fig. 8. Cumulative sand thickness for each CPT expressed as the height of bar and division in dense, moderate dense, and loose sand (colours) for the top 20 m from the surface. (A) For Naaldwijk Formation and (B) for units of Pleistocene age (Boxtel, Eem and Peelo Formations, Schaarsbergen Member (Drente Formation) and Urk Formation – Tynje Member).

Figure 2.7.2 Sand thicknesses with densities of the Naaldwijk formation and Pleistocene formations; Boxtel, Eem, Peelo, Drente and Urk (Kruiver et al., 2017)

3. Liquefaction assessment

3.1 Cone penetration test

From around 1917 rods were used to probe the underground with the goal of detecting harder and softer soils. Only in 1932 the cone penetration test was officially introduced in the Netherlands. Since then the CPT has undergone many alterations. Figure 3.1.1 shows a CPT that was done manually by Delft Geotechnics (Lunne et al, 1997).

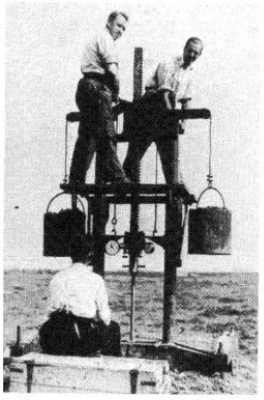

Figure 3.1.1 CPT manually done by Delft Geotechnics (Lunne et al, 1997)

The cone penetration test is a test by which a cone is pushed into the subsurface, see figure 3.1.2. The CPT can measure two important parameters, the cone resistance and the sleeve friction. The cone resistance is calculated by the total force on the cone divided by the area of the cone (Lunne et al, 1997). Moreover, the tip resistance gives an indication for the density (Deltares, 2016). The sleeve friction is calculated by the amount of force required to push the sleeve through the soil divided by the surface area of the friction sleeve (Lunne et al, 1997). Then, the friction ratio can be calculated with these two measured parametres, the ratio between the sleeve friction and tip resistance (USGS, 2019). More advanced CPTs can measure more parameters, such as the water pressure.

CPT is a relatively cheap technique to acquire information on the soil characteristics. (Vertek, 2014). The main benefit of CPTs is that they are very accurate at measuring the variability in the soil layers. Additionally, the CPT is repeatable, which increases the validity of the results. Furthermore, CPT data is easily available of Groningen provided by DINOloket (Deltares, 2016).

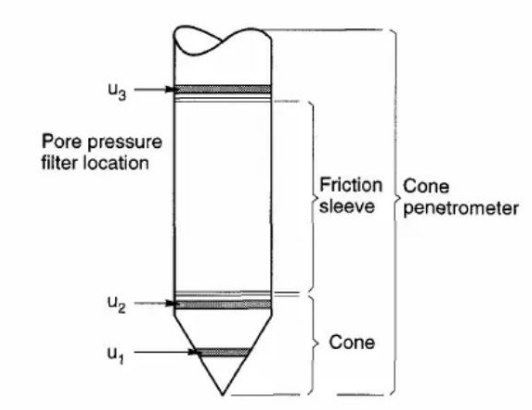

Figure 3.1.2 Cone penetrometer (Lunne et al, 1997)

3.2 Soil classification

The friction ratio and cone resistance data were used to define the soil type. It is generally known that layers with high friction ratios consist of clayey or peaty soils and layers with low values are made of sandy soils. Moreover, sands have a high cone resistance compared to clays (Vertek, n.d.). The cone resistance and friction ratio data were applied to two classification systems.

Firstly, a soil classification chart was used, see figure 3.2.1. The classification is based on the cone resistance and friction ratio values. In total there are 12 regions that represent soil units. Moreover, the graph gives information on increasing values of OCR, drainage (Dr) and sensitivity (S_t) (Robertson et al, 1986).

Secondly, for good measure a classification from a Dutch geotechnical report was used, see figure 3.2.2. This classification system was based on the cone resistance and friction ratio values. This was convenient since it shows how the Dutch classify their own soils. Furthermore, the Robertson was more precise and had no overlapping soil classes unlike the ATAR Geotechniek classification.

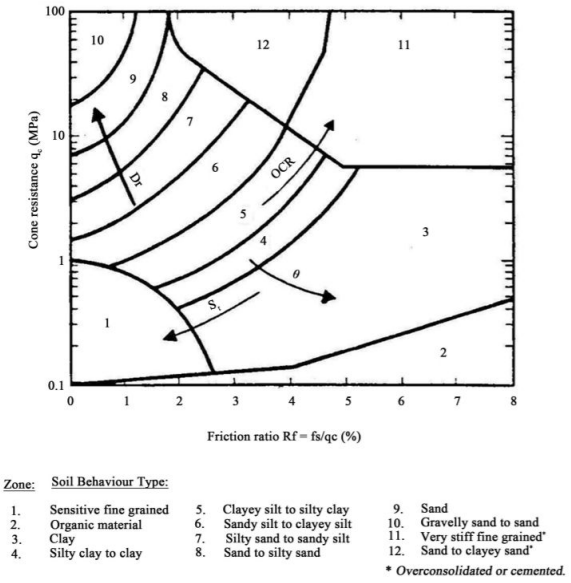

Figure 3.2.1 Soil classification chart (Robertson et al, 1986)

Grondsoort	Conusweerstand [MPa]	Wrijvingsgetal in [%]
grind	> 10	0,2 - 0,5
grof zand	> 10	0,4 - 0,6
zand	> 5	0,6 - 1,0
zand, siltig	> 4	0,8 - 1,4
zand, kleiig	> 2	1,0 - 2,0
leem	1 – 3	2,0 - 4,0
klei, vast	0 – 8	2,0 - 4,0
klei, matig	0 – 4	3,0 - 5,0
klei, slap	0 – 2	4,0 - 6,0
potklei	2 – 5	5,0 - 7,0
venige klei	0 – 6	5,0 - 8,0
veen	0 – 4	5,0 - 10,0

Figure 3.2.2 Soil classification, below groundwater (ATAR Geotechniek, 2016)

3.3 Soil behaviour index

The soil behaviour index helps to determine the liquefaction potential. First the normalized cone resistance (Q) and normalized friction ratio (F) must be calculated, see figure 3.3.1. The normalized cone resistance consists of the cone resistance, the vertical stress, the effective vertical stress, the n exponent and the reference stress (P_a). The cone resistance can be acquired from the CPT data. The vertical and effective vertical stress can be calculated with the taught material from the 'Soil Mechanics AESB2330 (2019)' course. Note that the soil is assumed to be fully saturated. The volumetric weight of the soil is needed to estimate the stresses and can be determined with the NEN 6740 table, that can be found in Appendix A2 by using the soil type and cone resistance value. The reference stress is a constant of 10 kPa. The n exponent is usually about 0.5 for sand to 1 for clays (Robertson & Wride, 1998). The Robertson methodology is to first set the n exponent to 1, even for sands (Robertson, 1990). If the I_c is larger than 2.6, the soil layer is not prone to liquefaction since it is deemed to be too rich in clay (Robertson & Wride, 1997). However, if the Ic is smaller or equal to 2.6 for sands, the process should be iterated with n equal to 0.5, this determines whether the soil layers are liquefiable. Furthermore, the normalized friction ratio contains the sleeve friction, the cone resistance and the vertical stress.

$$I_c = \left[\left(3.47 - \log(Q)\right)^2 + \left(1.22 + \log(F)\right)^2 \right]^{0.5}$$

$$Q = \left(\frac{q_c - \sigma_{vc}}{P_a} \right) \left(\frac{P_a}{\sigma'_{vc}} \right)^n$$

$$F = \left(\frac{f_s}{q_c - \sigma_{vc}} \right) \cdot 100\%$$

F	normalized friction ratio [dimensionless]
Q	normalized cone resistance [dimensionless]
q_c	tip resistance [MPa]
f_s	sleeve friction [MPa]
σ_{vc}	vertical stress [MPa]
σ_{vc}'	effective vertical stress [MPa]
P_a	reference stress [MPa]
n	exponent [dimensionless]

Figure 3.3.1 Soil behaviour index equations with legend (Robertson & Wride, 1997)

Liquefaction case histories based on Q and F

The figure 3.3.2 is another CPT soil classification chart with data from case histories where liquefaction has or has not been observed (Robertson, 1990). The classification depends on the Q and F and there are in total 9 regions that represent the classes. Furthermore, the chart indicates increasing values for the sensitivity, OCR and age. Liquefaction occurred under a normalized cone tip resistance of 150 MPa. Furthermore, cases that have similar positions in figure 3.3.2, can have very different outcomes in terms of liquefaction or no liquefaction. This shows that there is more at play other than the Q and F factors that can lead to liquefaction.

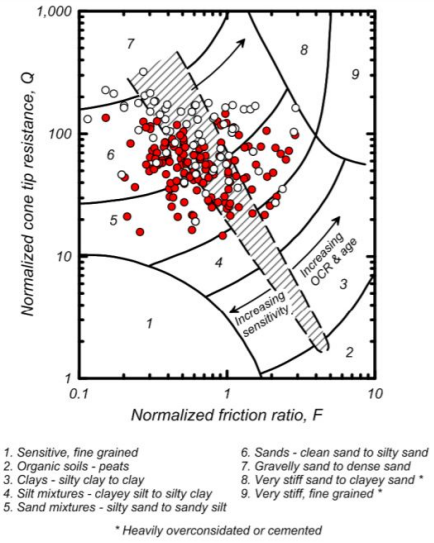

Figure 3.3.2 CPT classification chart; red bullets, liquefaction, white dots, no liquefaction (Boulanger & Idriss, 2014; Robertson, 1990)

Correlation between the I_c and fines content

The percentage of fines play a role in the liquefaction sensitivity. Two groups of researchers have investigated the relation between the I_c and the fines percentage. The results are shown in figure 3.3.3. It turns out that with knowing the I_c and fines content, an assumption can be made on whether liquefaction will take place. However, this is based on data from case histories, making it an empirical relation. Though, it can be seen that low values of Ic in between 1 and 1.7 and fines content from 5-30% are liquefaction free cases.

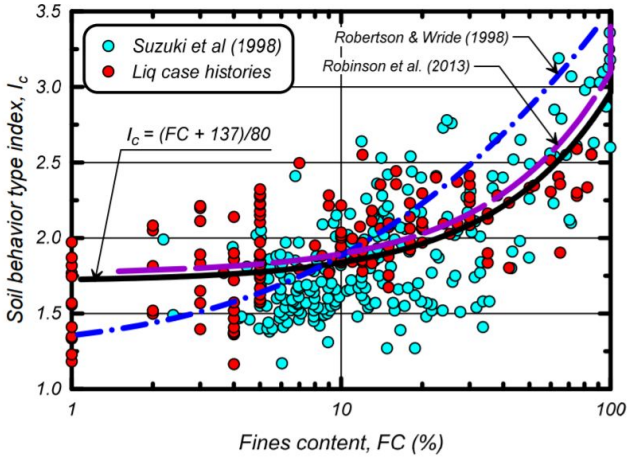

Figure 3.3.3 Relation between Ic and fines content (Boulanger & Idriss, 2014)

3.4 r_d and MSF

Depth stress reduction coefficient

The depth stress reduction factor is "an empirical factor that accounts for the non rigid response of the soil" (NAM, 2018). The r_d parameter is dependent on the depth and the magnitude of the earthquake. Figure 3.4.1 shows the formulae that describe the depth stress reduction factor. In the formulae z stands for the depth below the ground in metres, M for the magnitude and the sinus is in radians (Boulanger & Idriss, 2014).

The closer the r_d is to 1 the larger the magnitude of the earthquake (Idriss, 1999). This can be seen in figure 3.4.2. In Groningen the induced earthquakes have so far not been larger than 3.6. Hence, the stress reduction coefficient would be close to 0.3 or perhaps below that.

$$r_d = \exp\left[\alpha(z) + \beta(z) \cdot M\right]$$

$$\alpha(z) = -1.012 - 1.126 \sin\left(\frac{z}{11.73} + 5.133\right)$$

$$\beta(z) = 0.106 + 0.118 \sin\left(\frac{z}{11.28} + 5.142\right)$$

Figure 3.4.1 r_d equations (Boulanger & Idriss, 2014)

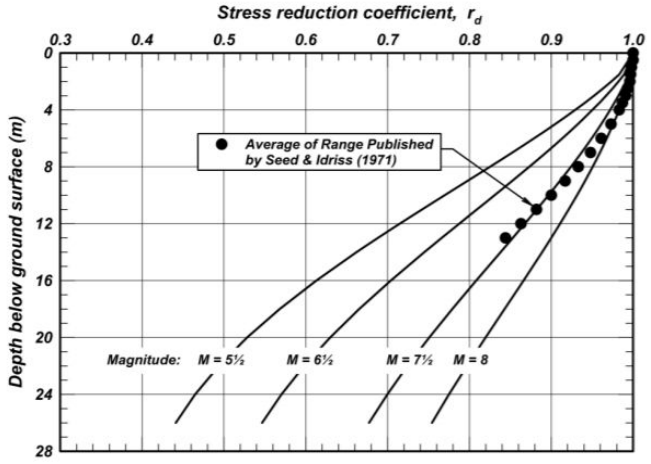

Figure 3.4.2 Relation between r_d and depth (Boulanger & Idriss, 2014)

Magnitude scaling factor

"Magnitude scaling factors account for the durational effects of the ground shaking on liquefaction triggering" (Kruiver et al, 2017, p. s227). This is important because it helps to understand the outcomes of earthquakes in different magnitudes. Figure 3.4.3 describes the MSF for sands. Since sands are prone to liquefaction, we want to know their MSF. The MSF solely depends on the magnitude of an earthquake (Boulanger & Idriss, 2014). The higher the magnitude the lower the MSF factor, see figure 3.4.4. Moreover, figure 3.4.5 shows the MSF

for sand and clay. The MSF for clay has a maximum value of 1.13 and sand a value of 1.8. Clay and sand react differently to ground shaking, because they have different soil characteristics.

$$MSF = 6.9 \cdot \exp\left(\frac{-M}{4}\right) - 0.058 \leq 1.8$$

Figure 3.4.3 MSF for sands; M is magnitude (Idriss, 1999)

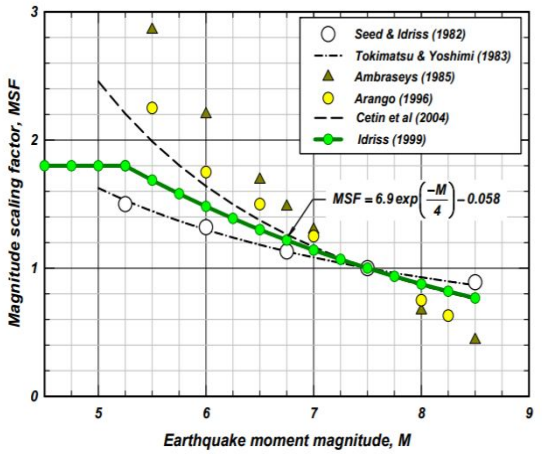

Figure 3.4.4 Relation between MSF and M for sands (Boulanger & Idriss, 2014)

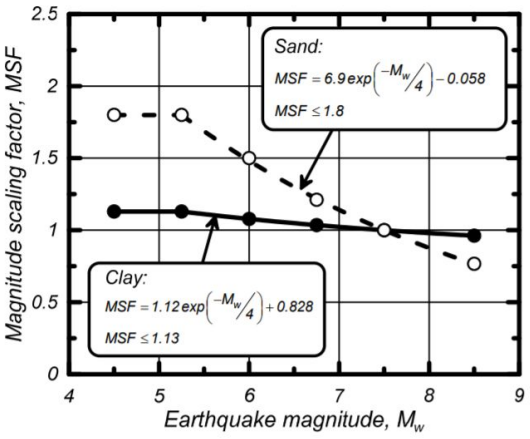

Figure 3.4.5 Relation between MSF and M for clays and sands (Boulanger & Idriss, 2007)

Factor of safety

The MSF can be used to calculate the factor of safety (FS). The FS is expressed in MSF, CSR and $CRR_{7.5}$, see equation 1 (Robertson & Wride, 1998).

$$FS = (CRR_{7.5}/CSR)MSF \quad (1)$$

The MSF calculations have been explained in the previous paragraph. Furthermore, the cyclic stress ratio (CSR) represents the seismic demand of the underground (Youd & Idriss, 2001). The CSR can be calculated with equation 2 (Youd & Idriss, 2001), see figure 3.4.6 for its legend.

$$CSR = (\tau_{av}/\sigma'_{vo}) = 0.65(a_{max}/g)(\sigma_{vo}/\sigma'_{vo})r_d \quad (2)$$

a_{max} = maximum horizontal acceleration at the ground surface
τ_c = cyclic shear stress
g= acceleration due to gravity
σ_v' = total effective vertical stresses
σ'_{vo} = initial effective vertical stresses
r_d = depth-stress reduction factor

Figure 3.4.6 Legend for CRS formula (Youd & Idriss, 2001)

$CRR_{7.5}$ stands for the cyclic resistance ratio that shows the ability of soil layers to resist liquefaction at a magnitude of 7.5. In order to adjust the $CRR_{7.5}$ for other magnitudes, the CRR must be multiplied by the MSF. The $CRR_{7.5}$ can be calculated with equations 3 and 4 (Robertson & Wride, 1998), it depends on the $(q_{c1N})_{cs}$ values.

$$\text{If } (q_{c1N})_{cs} < 50 \quad CRR_{7.5} = 0.833[(q_{c1N})_{cs}/1{,}000] + 0.05$$
$$\text{If } 50 \leq (q_{c1N})_{cs} < 160 \quad CRR_{7.5} = 93[(q_{c1N})_{cs}/1{,}000]^3 + 0.08 \qquad (3 \& 4)$$

$(q_{c1N})_{cs}$ stands for the equivalent clean sand resistance of silty sands, which can be determined with the q_{c1N} and K_c, see equation 5 (Robertson & Wride, 1998).

$$(q_{c1N})_{cs} = K_c q_{c1N} \qquad (5)$$

The q_{c1N} stands for the normalized penetration resistance for clean sands and the K_c is the correction factor for grain characteristics. The K_c depends on the I_c value, see equations 6 and 7.

$$\text{for } I_c \leq 1.64 \quad K_c = 1.0 \qquad (6)$$

$$\text{for } I_c > 1.64 \quad K_c = -0.403I_c^4 + 5.581I_c^3 - 21.63I_c^2 + 33.75I_c - 17.88 \qquad (7)$$

CRS and q_{c1N}

Many research teams have shown the relation between the CSR and the cone tip resistance, see figure 3.4.7. There is a clear threshold between the liquefaction and non liquefaction cases. Relatively low tip resistance combined with higher cyclic stress ratio results in liquefaction.

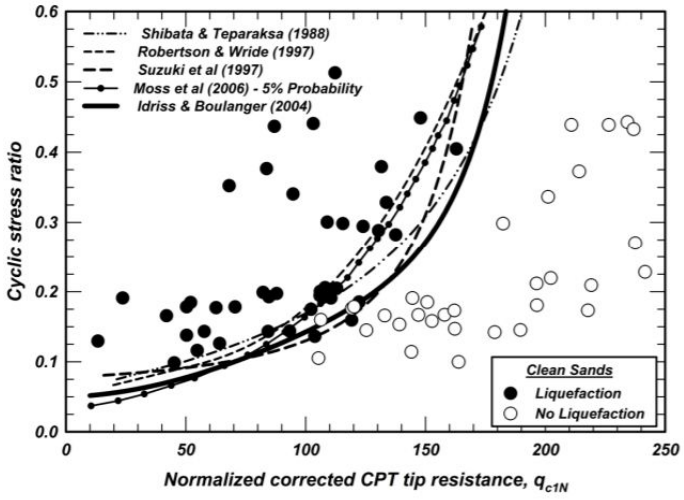

Figure 3.4.7 Correlation between the CSR and q_{c1N}; for M=7.5 and σ'_v= 1 atm (Idriss & Boulanger, 2008)

3.5 r_d and MSF altered for Groningen case

Recent research commissioned by 'Nederlands Aardolie Maatschappij' (NAM), produced an alternative way to calculate r_d and MSF which are more applicable to Groningen. The international definitions of the r_d and MSF are based on case studies that are very different to the circumstances in Groningen. The earthquakes have a low magnitude, but occur in the shallow underground leading to great damage at the surface. The difference lies in the magnitude and depth of the earthquakes as well as the density and depth of the liquefiable soil layers. Moreover, data was needed from cases that were similar to the Groningen condition. The New Zealand liquefaction case histories turned out to be the most similar (Green et al, 2018).

Furthermore, the NAM study applied their new methodology to a pilot study area in the northern part of the Groningen gas field. The study area had the following three conditions: "the largest shaking hazard, thick shallow young loose sands and multiple site response zones" (Green et al, 2018). Here, the site response indicates the site response to the ground shaking that is triggered by an earthquake (Kruiver et al, 2015).

The study area contains sands of Naaldwijk that have been identified as most prone to liquefaction. Figure 3.5.1 shows the study area in the rectangular box and the thicknesses of the sand compositions of the Naaldwijk formation (Green et al, 2018).

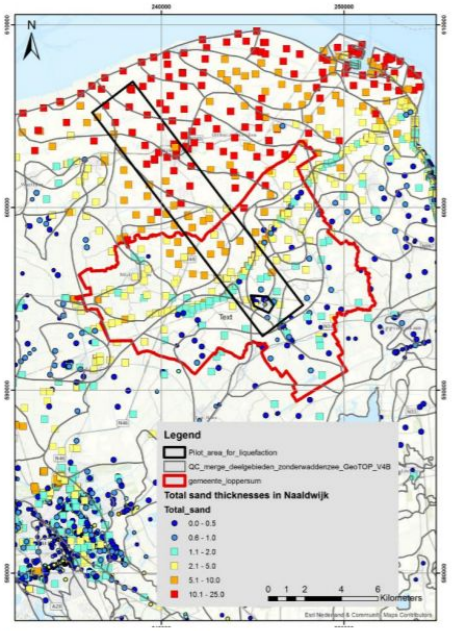

Figure 3.5.1 Sand thicknesses of Naaldwijk and the location of the study area (Green et al, 2018)

Groningen specified r_d

The following r_d was developed, see equations 8, 9 and 10. β_i stands for regression coefficients and A_{rd} is the asymptotic level for the r_d at depth or in other words r_d is defined as '1 - A_{rd}' as z goes to infinity. Moreover, the heteroscedastic standard deviation of the r_d can be calculated with equation 11. In these equations a_{max} is in g units, V_{s12} in metres per second and z in metres (Green et al, 2018).

$$r_{d-Gron} = 1 - \frac{A_{rd}}{1+exp\left[-\frac{\ln(z)-(\beta_2+\beta_6 \cdot \boldsymbol{M})}{(\beta_3+\beta_7 \cdot \boldsymbol{M})}\right]};\ 0 \leq r_d \leq 1 \tag{8}$$

$$A_{rd} = \beta_1 + \beta_4 \cdot \min[\boldsymbol{M}, 6.5] + \beta_5 \cdot \ln(a_{max}) + \beta_9 \cdot V_{s12};\ \text{for } a_{max} \leq 0.3\ \text{g} \tag{9}$$

$$A_{rd} = \beta_1 + \beta_4 \cdot \min[\boldsymbol{M}, 6.5] + \beta_5 \cdot \ln(a_{max}) + \beta_8 \cdot \ln\left(\frac{a_{max}}{0.3}\right) + \beta_9 \cdot V_{s12};\ \text{for } a_{max} > 0.3\ \text{g} \tag{10}$$

$$\sigma_{r_d} = \frac{\beta_{10}}{1 + exp\left[-\frac{\ln(\max[z, 5]) - (\beta_2 + \beta_6 \cdot \boldsymbol{M})}{(\beta_3 + \beta_7 \cdot \boldsymbol{M})}\right]} \tag{11}$$

Groningen specified r_d compared to

Figure 3.5.2 shows graphs that represent the r_d versus depth relations from different studies, each graph goes with a different magnitude. Also different values for the a_{max} are shown for the Groningen specific r_d (Green et al, 2018).

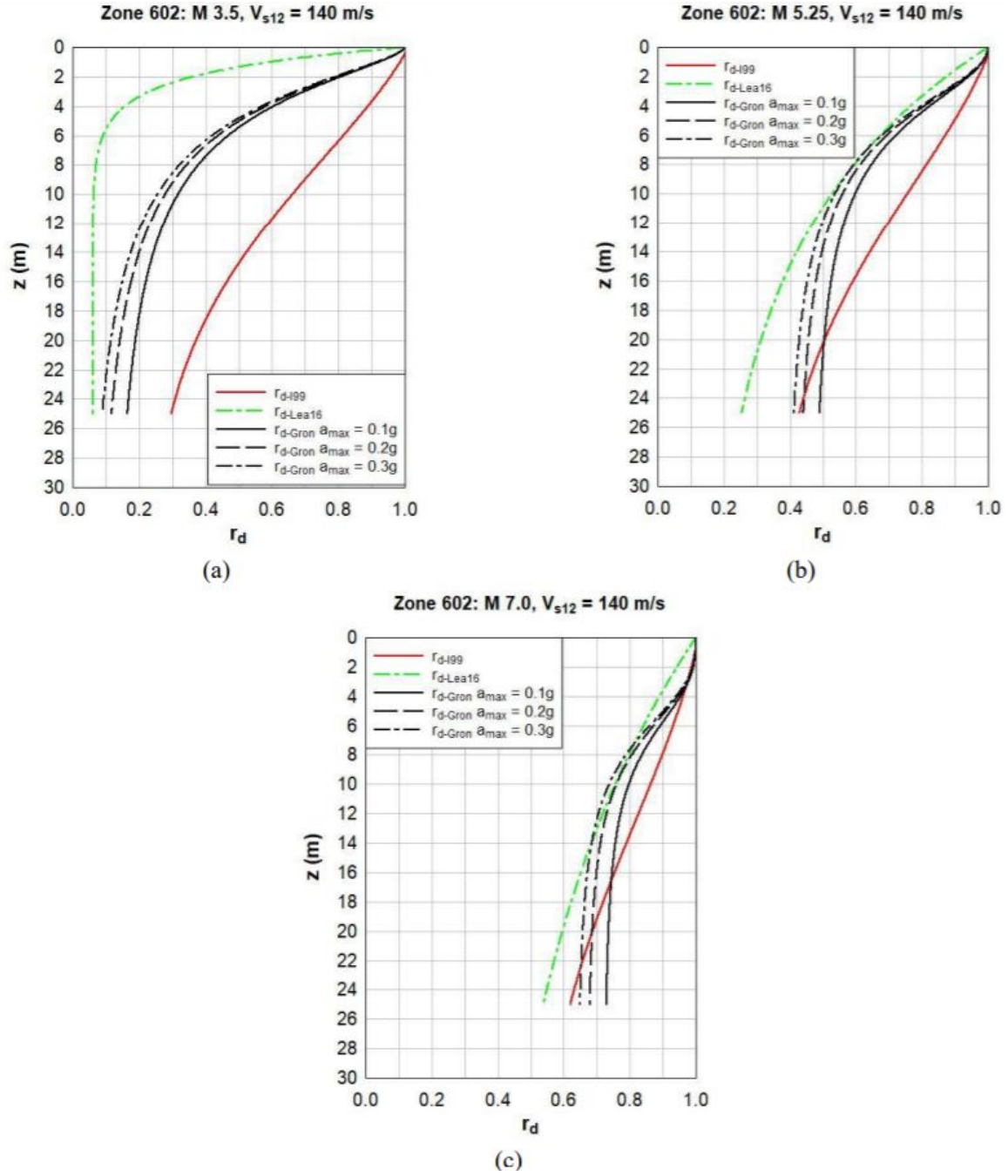

Figure 3.5.2 r_d and depth relations; (a): M 3.50, (b): M 5.25, (c): M 7.00. ; green= Lasley et al. (2016), red= Idriss (1999), black= Green et al. (2018) and for different a_{max} values.

Groningen specified n_{eq} and MSF

The n_{eq} is a part of the equation that defines the magnitude scaling factor. The only new parameters are the M which stands for the magnitude and α_i stands for the regression coefficients (Green et al, 2018).

$$ln\left[n_{eqM-Gron}(\boldsymbol{M}, a_{max}, V_{s12})\right] = \alpha_1 + \alpha_2 \cdot \ln(a_{max}) + \alpha_4 \cdot \boldsymbol{M} + \alpha_5 \cdot V_{s12}; \quad \text{for } a_{max} \leq 0.3\ \text{g} \tag{12}$$

$$ln\left[n_{eqM-Gron}(\boldsymbol{M}, a_{max}, V_{s12})\right] = \alpha_1 + \alpha_2 \cdot \ln(a_{max}) + \alpha_3 \cdot \ln\left(\frac{a_{max}}{0.3}\right) + \alpha_4 \cdot \boldsymbol{M} + \alpha_5 \cdot V_{s12};\ \text{for } a_{max} > 0.3\ \text{g} \tag{13}$$

The MSF with its standard deviation is defined as follows:

$$MSF_{Gron} = \left\{\frac{7.25}{n_{eqM-Gron}(\boldsymbol{M}, a_{max}, V_{s12})}\right\}^{0.34} \leq 2.04 \tag{14}$$

$$\sigma_{\ln(MSF_{Gron})} = 0.34 \cdot \sigma_{\ln(n_{eqM-Gron})} \tag{15}$$

The following graph shows the relationship between the MSF and M (magnitude). The graph shows the MSF_{Gron} and MSF_{WUS}, these are represented with different a_{max} values. The MSF_{WUS} was made with the most commonly used MSF that was developed by Boulanger and Idriss. The MSF_{Gron} and MSF_{WUS} are very similar to each other. The only difference between these two relations is that for the MSF_{WUS} the a_{max} has more influence. Furthermore, the graph also displays the MSF_{IB08}, which is the original MSF developed by by Idriss and Boulanger. Overall, the MSF_{IB08} has much larger values for magnitudes lower than 7. Moreover, as the magnitude decreases the MSF_{IB08} value becomes more overpredicted (Green et al, 2018). Besides that, the MSF_{IB08} is unlike the other relations nonlinear.

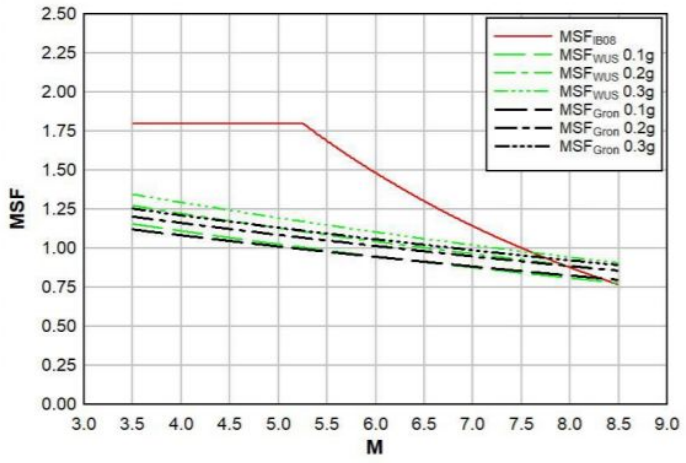

Figure 3.5.3 MSF and M correlations; green from Green et al. (2018) & for different a_{max} values, red from Boulanger & Idriss (2014), black from Green et al. (2018) & for different a_{max} values

Liquefaction potential index

The area most prone to liquefaction was determined with the liquefaction index potential (LPI). The LPI is defined as an integral and depends on the FS_{liq}, F_{LPI} , w(z) and depth, see equation 16. FS_{liq} is "the factor of safety against liquefaction triggering". The F_{LPI} is a parameter that depends on the $FS_{liq.}$ The F_{LPI} is equal to 0 for $FS_{liq} \geq 1$ and F_{LPI} is 1- FS_{liq} for $FS_{liq} < 1$. The w(z) represents the depth weighing function that is define das w(z)=10-0.5z, where z is the depth in metres below the ground level (Green et al, 2018).

$$LPI = \int_0^{20\,m} F_{LPI}(FS_{liq}) \cdot w(z)dz \quad (16)$$

Result of the NAM study

Most of the LPI results of the pilot study were below five, meaning no to minor surficial liquefaction manifestations. Only sites in Zandeweer had LPI values above five, indicating moderate surficial liquefaction manifestations. An LPI that indicates severe surficial liquefaction manifestations was not detected anywhere. Zandeweer had the highest risk of liquefaction, see figure 3.5.4. Moreover, Zandeweer is located in an area where the sands of the Naaldwijk formation are very thick, about 5.1 to 25 metres (Green et al, 2018), which is a clear indicator for liquefaction.

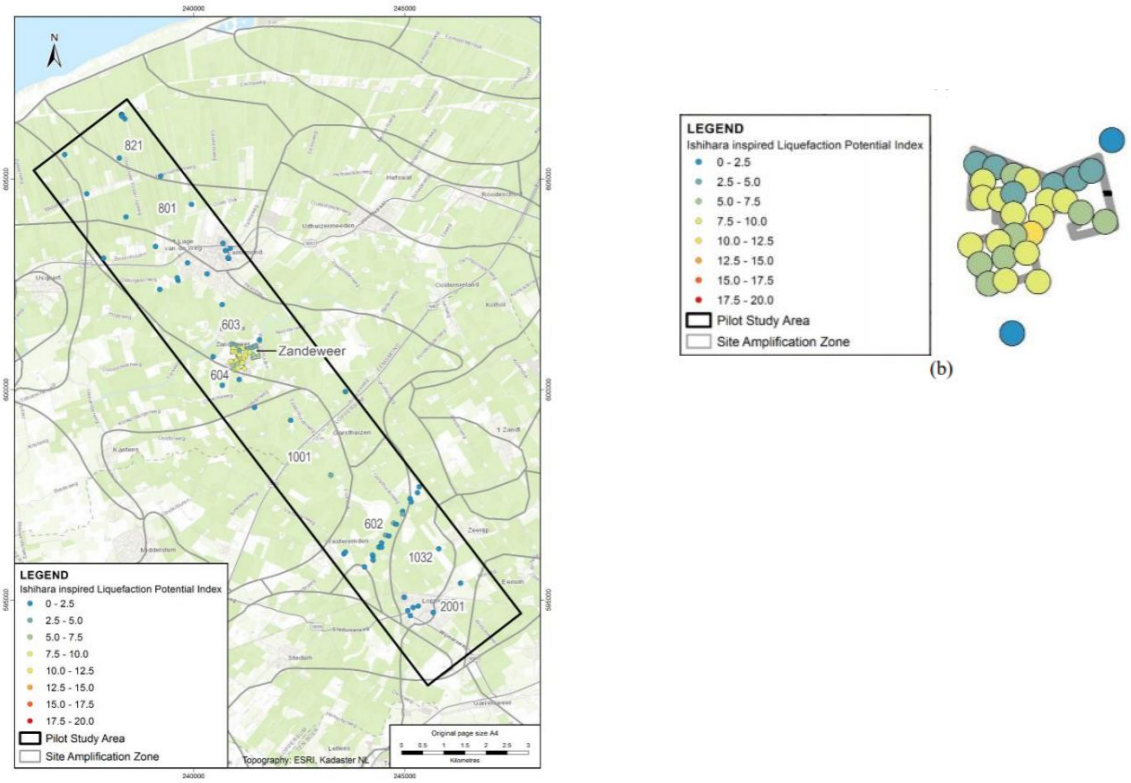

Figure 3.5.4 LPI of the study area with legend (Green et al, 2018)

Zandeweer

Figure 3.5.5 shows the position of Zandeweer on the Naaldwijk formation thickness map. Zandeweer is located in the relatively thick Naaldwijk formation zone, which supports the results of the NAM study.

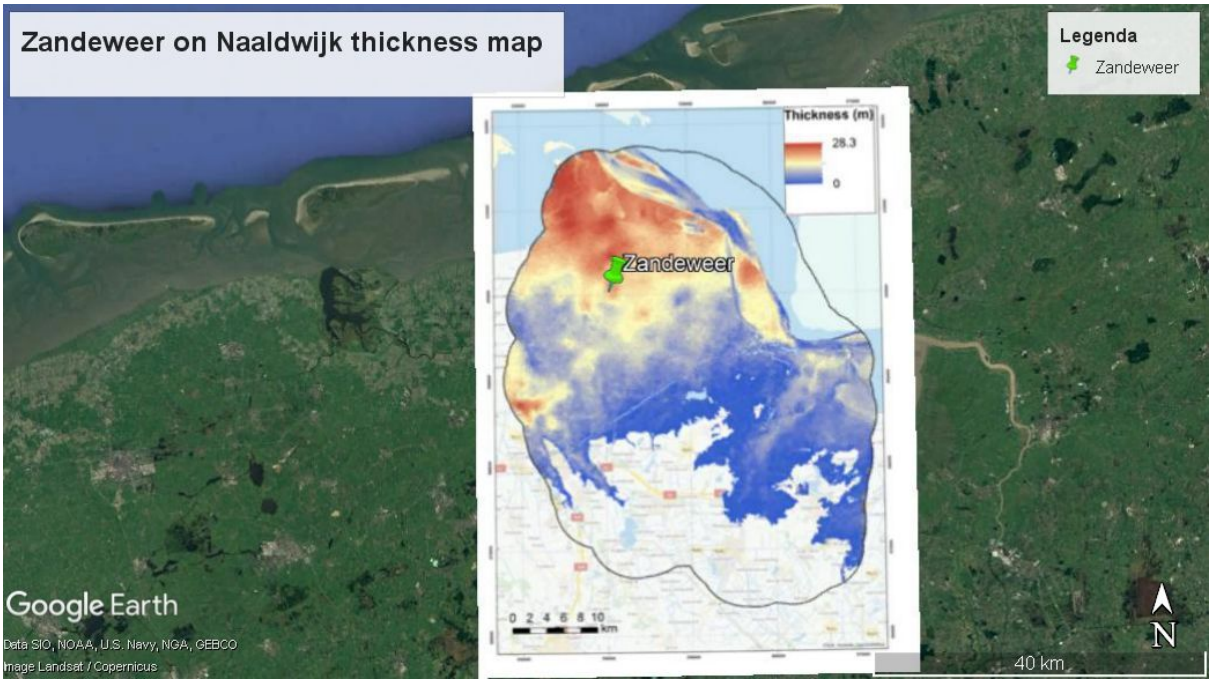

Figure 3.5.5 Zandeweer on Naaldwijk thickness map made in Google Earth; GeoTOP 3D subsurface model (Maljers et al, 2016)

Furthermore, Zandeweer is located in a low to moderate PGA value region, see figure 3.5.6. Thus, an earthquake in Zandeweer would cause a low to moderate amount of damage compared to Ten Boer for example, based on the seismic hazard map.

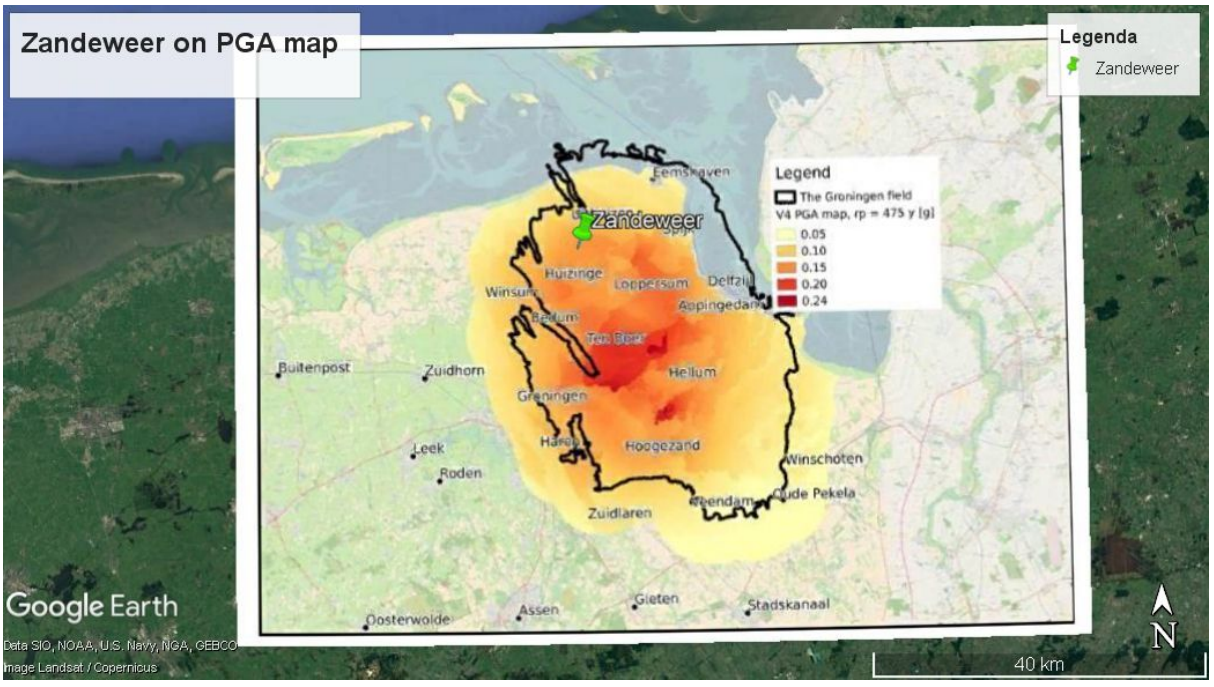

Figure 3.5.6 Zandeweer superimposed on the seismic hazard map made in Google Earth (KNMI, n.d.)

4. Liquefaction assessment for three terpen in Groningen

4.1 Terpen selection

A CPT analysis was performed to three terpen, these were found with the use of AHN Viewer, Actueel Hoogtebestand Nederland. This is a website that shows the elevation map of the Netherlands. In order to find the ground level height, that exclude high buildings and infrastructure, use the option 'Lijst met lagen', 'AHN2- maaiveld (Dynamische opmaak)'. Then looking for round objects that are more red or orange compared to its yellow and blue surroundings. The last step is to determine with DINOloket, whether there is available CPT data.

The three chosen terpen are Middelstum, Beswerd and Wirdum. They are located in the Northern part of the Groningen gas field region, figure 4.1.1 shows their position. It would have been nice to have a terp in the southern part. Though, there were barely any terpen there, even less terpen with the appropriate CPT data.

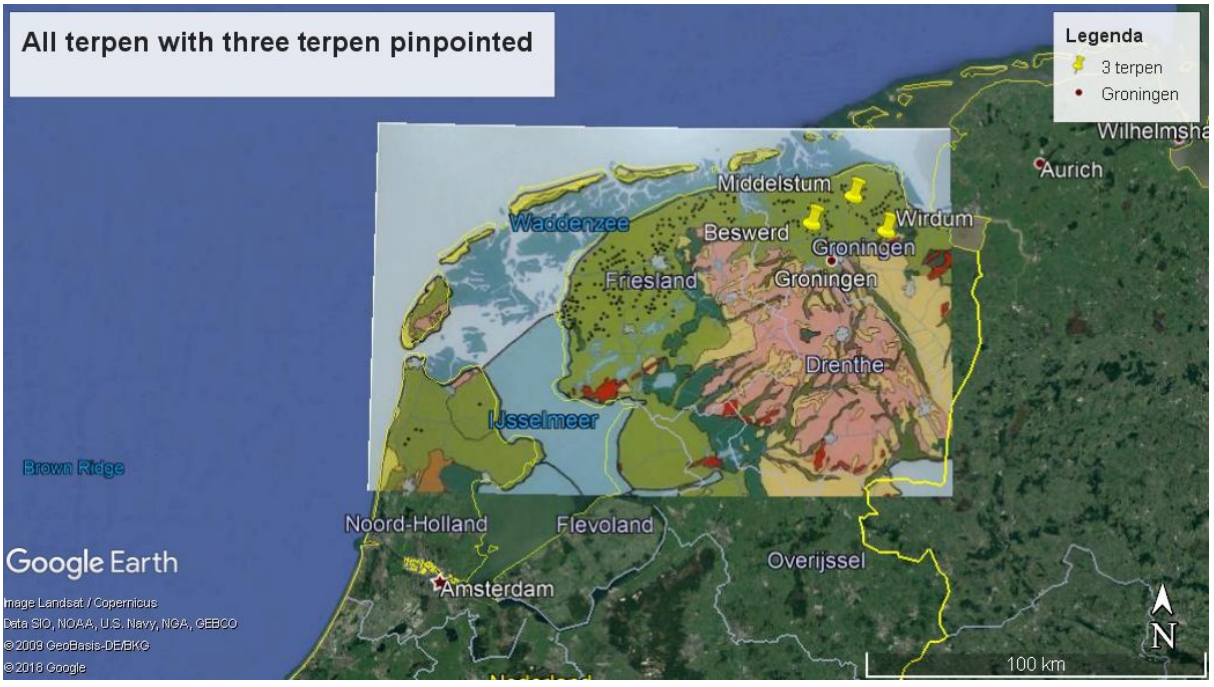

Figure 4.1.1 Three terpen superimposed on the Dutch terpen map made in Google Earth; black dots represent terpen (Picture of map in Museon, n.d.)

4.2 Background information terpen

Middelstum is a village in Loppersum, Groningen. It is special because of its radial terp structure, which can be seen in figure 4.2.1. Middelstum had 2030 villagers in 2018 (AlleCijfers, 2016). This is an interesting terp, because it is close to Zandeweer and located in the high PGA value region. Middelstum owns several national monuments, including terp remains (Rijksmonumenten, n.d.).

Figure 4.2.1 Middelstum aerial view (Beeldbank Nederland, 2015)

Beswerd is a township in Westerkwartier, Groningen. The township contains two farms and some workers houses and there are another two farms nearby, see figure 4.2.2. Beswerd is assumed to have about 15 residents (Plaatsengids, n.d.). Beswerd has not been classified as a national monument and has not been identified as an AMK.

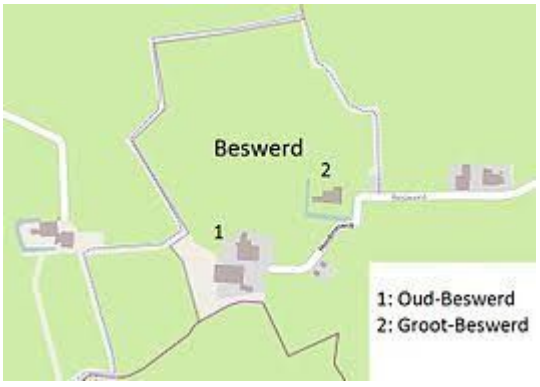

Figure 4.2.2 Map of Beswerd (Openstreetmap, 2019)

Wirdum is also a village in Loppersum in the province Groningen. Nowadays Wirdum has about 130 houses and 320 villagers. The village contains six national monuments, including terpen (Plaatsengids, n.d.). Figure 4.2.3 shows a terp that is located in Wirdum.

Figure 4.2.3 Terp in Wirdum, Groningen (RCE, 2007)

4.3 Data on the subsurface of three terpen

Borehole data

The borehole data of the Middelstum terp is located on the terp. The first four metres are composed of clay and fine sand from the Naaldwijk formation, see figure 4.3.1. The borehole closest to the Beswerd terp gives information about the first six metres. The data is similar to the Middelstum terp and contains clay and fine sand from the Naaldwijk formation, see figure 4.3.2. Lastly, the Wirdum borehole data covers the first five metres and the borehole log profile is made up of clay and some peat, see figure 4.3.3. The clay comes from the Naaldwijk formation and the peat from the Nieuwkoop formation. The Middelstum and Beswerd terp both contain fine sands, this increases their chance of liquefaction. Moreover, the borehole data location can be seen in Appendix B1.

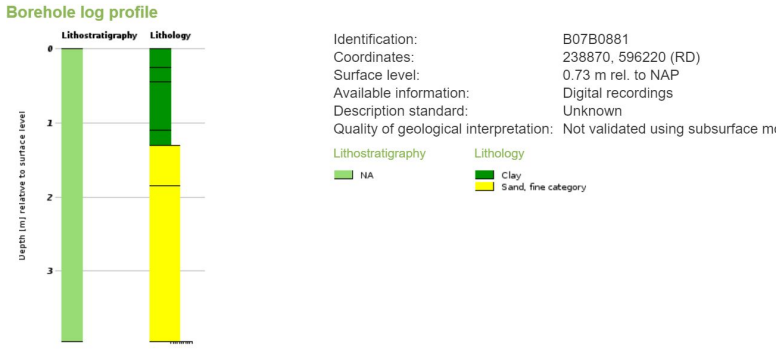

Figure 4.3.1 Middelstum borehole log profile

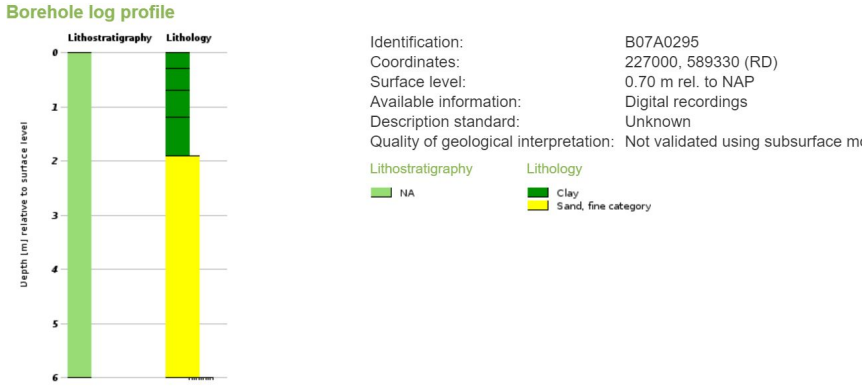

Figure 4.3.2 Beswerd borehole log profile

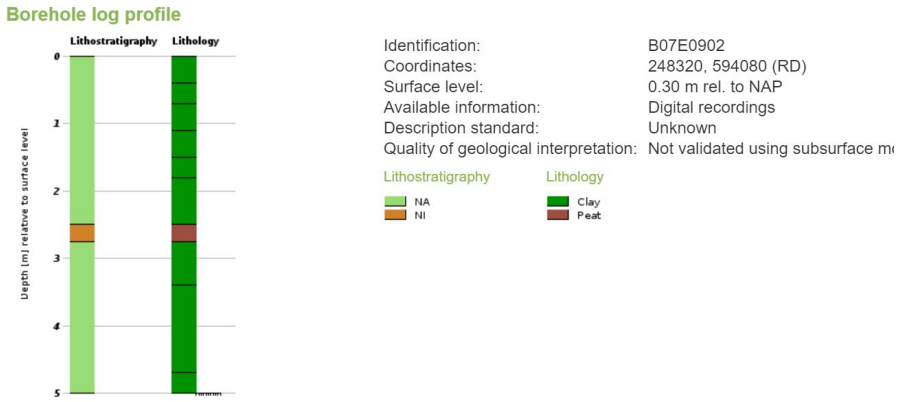

Figure 4.3.3 Wirdum borehole log profile

Naaldwijk sand densities of three terpen

Of all the three terpen Middelstum has the highest amount of Naaldwijk sand, according to figure 4.3.4. Beswerd can have some Naaldwijk sand and Wirdum has none. Moreover, Middelstum has more loose sands compared to Middelstum.

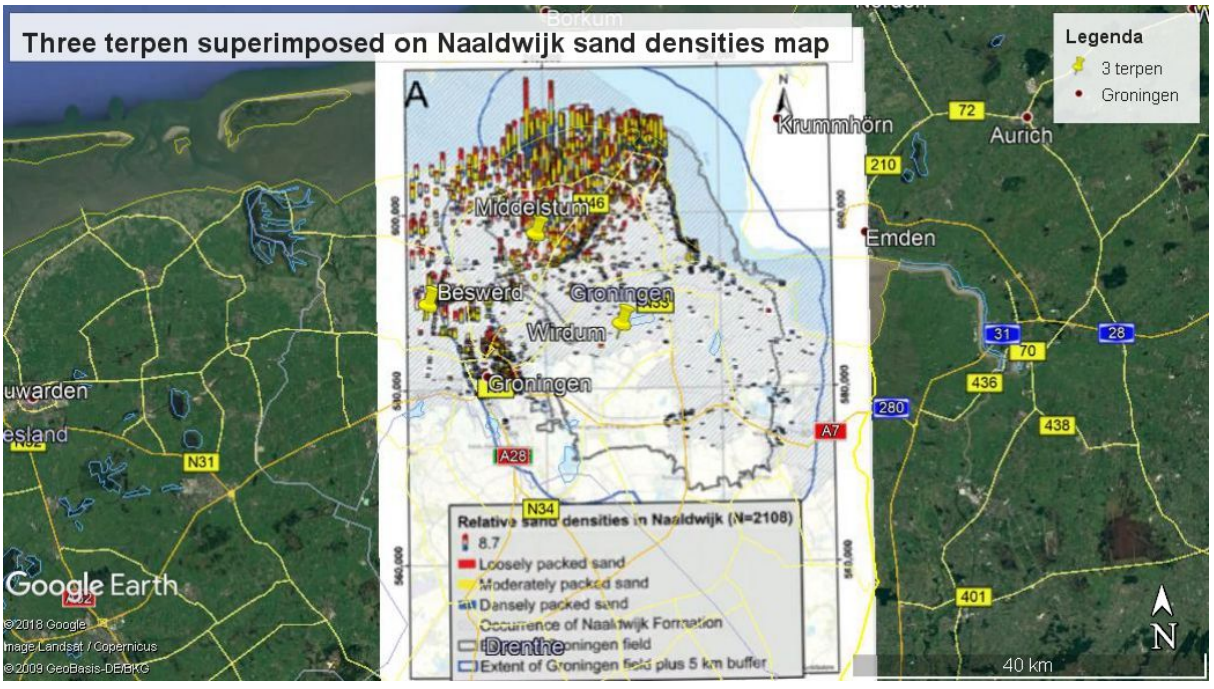

Figure 4.3.4 Three terpen superimposed on Naaldwijk formation sand densities map with Google Earth (Kruiver et al., 2017)

Naaldwijk formation thickness of three terpen

Furthermore, Middelstum is positioned in an area with a low to moderate amount of the Naaldwijk formation, see figure 4.3.5. Wirdum has a thin layer of Naaldwijk. Lastly, Beswerd is located outside of the map so the thickness is unknown based on figure 4.3.5.

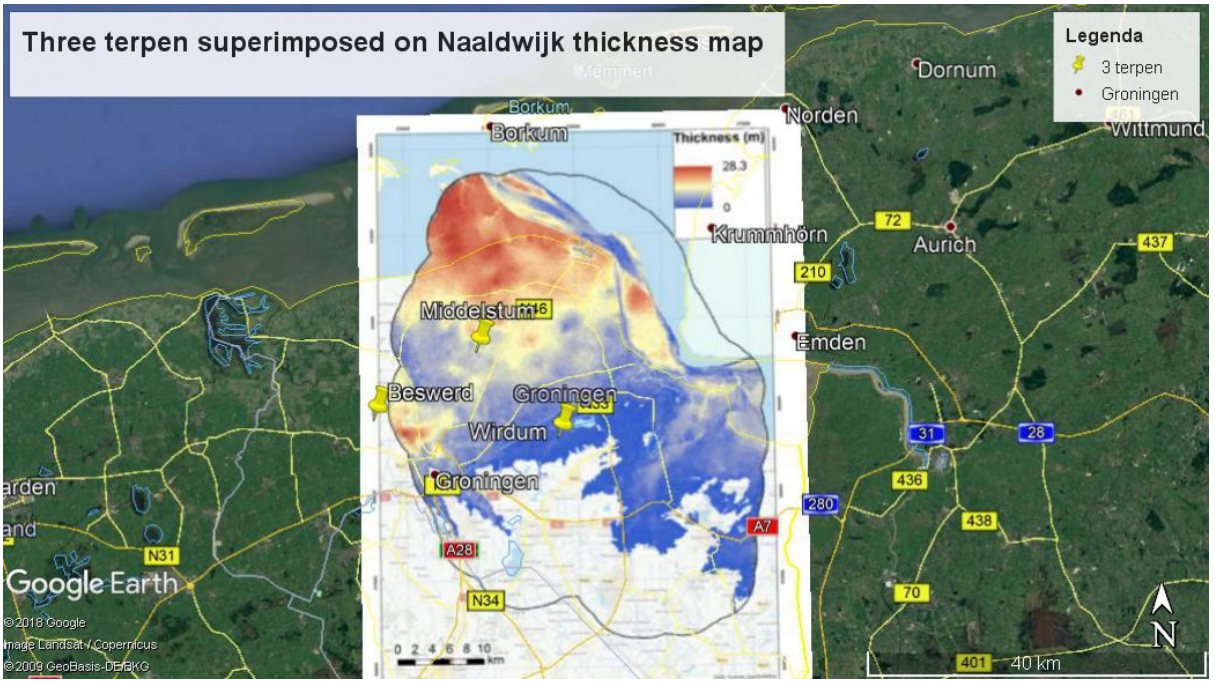

Figure 4.3.5 Three terpen superimposed on Naaldwijk formation thickness map with Google Earth (Kruiver et al., 2017)

Position of the terpen on the seismic hazard map

Wirdum is located in a high PGA region and Middelstum in the low to moderate region, according to figure 4.3.5. Beswerd is positioned outside of the map and also outside of the Groningen gas field region. Hence, it is safe to say, that it is in a low PGA environment.

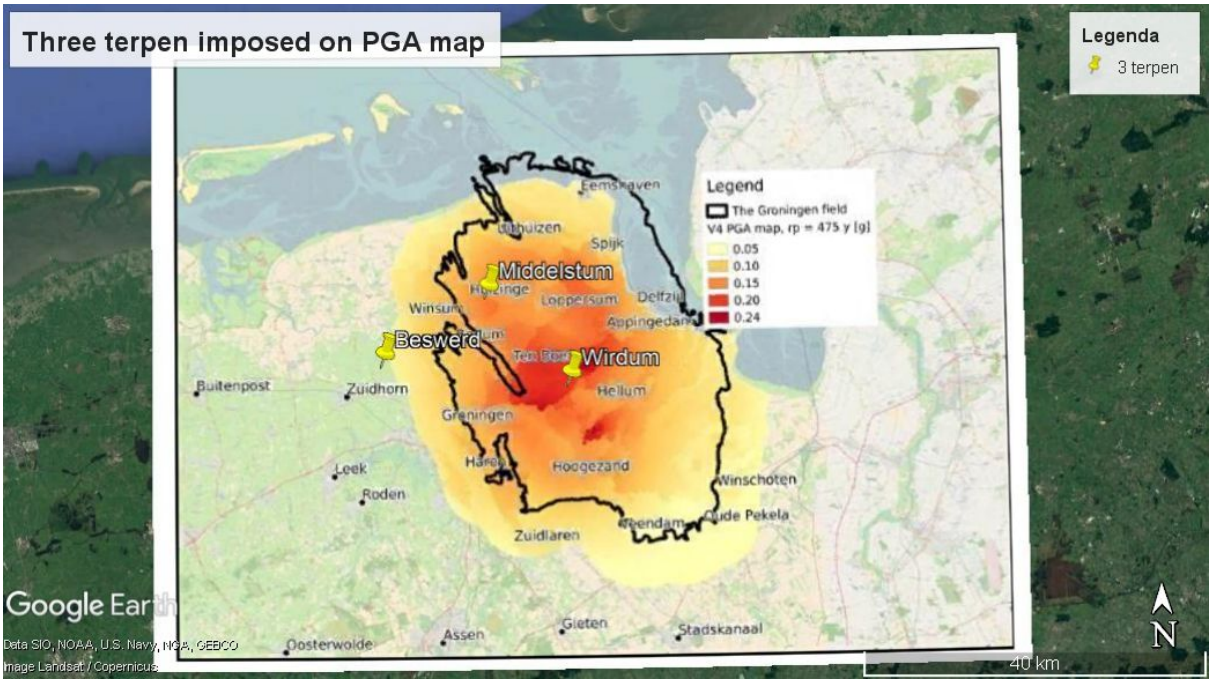

Figure 4.3.6 Three terpen superimposed on seismic hazard map made with Google Earth (KNMI, n.d.)

4.4 CPT data from DINOloket

The terpen that were chosen had to fulfill several requirements. First off, CPT data must be available preferably a CPT that took place on the terp or a maximum distance of 20 metres away from the terp. The further away the test was done, the less accurately the CPT data would represent the soil of the terp, since there is a high heterogeneity in the subsurface.

Furthermore, the CPT data was supplied by DINOloket. DINOloket offers free data and information on the Dutch underground, such as borehole data and geological cross sections. The CPT data from DINOloket do not all have the same quality. DINOloket states that older data are less accurate compared to recent data, especially the data before 1982 is of a lower quality (Dinoloket, n.d.). Hence, another condition for the CPT data of a terp is to be from after 1982. Moreover, the precise location of the collected CPT data is shown in Appendix B1.

The Dinoloket provided graphs of the friction ratio, cone resistance and the sleeve friction, the graphs can be found in Appendix B2. Dinoloket also supplied GEF files at request that contained the data of these graphs. These GEF files were imported in Excel. So the I_c parameter could be calculated per soil layer.

Moreover, the first and last values of the sleeve friction dataset were not realistic, this probably had to do with the mechanics of the machine. Hence, the same went for the friction ratio, because it includes the sleeve friction values. The unrealistic values of 999.9 were changed to 0 and not include into the average calculations so that these anomalies would not affect the rest of the results.

4.5 2D visualisation of AHN data of terpen with AHN Viewer

2D images of the terpen were produced from north to south and east to west with AHN2 data in the AHN viewer. Figure 4.5.1 shows the legend for the AHN images.

The Middelstum terp has more or less shallow slopes in figure 4.5.2. When looking at the north to south cross section, the overall shape looks stable. The Beswerd terp has sharper slopes that are shaped more gradual in the west to east cross section, see figure 4.5.3. Lastly, the Wirdum terp in figure 4.5.4 has an irregular shape. The west to east cross section of the terp seems to have a gap in it, this might be the cause of some type of damage.

Figure 4.5.1 AHN legend from low (blue) to high (red)

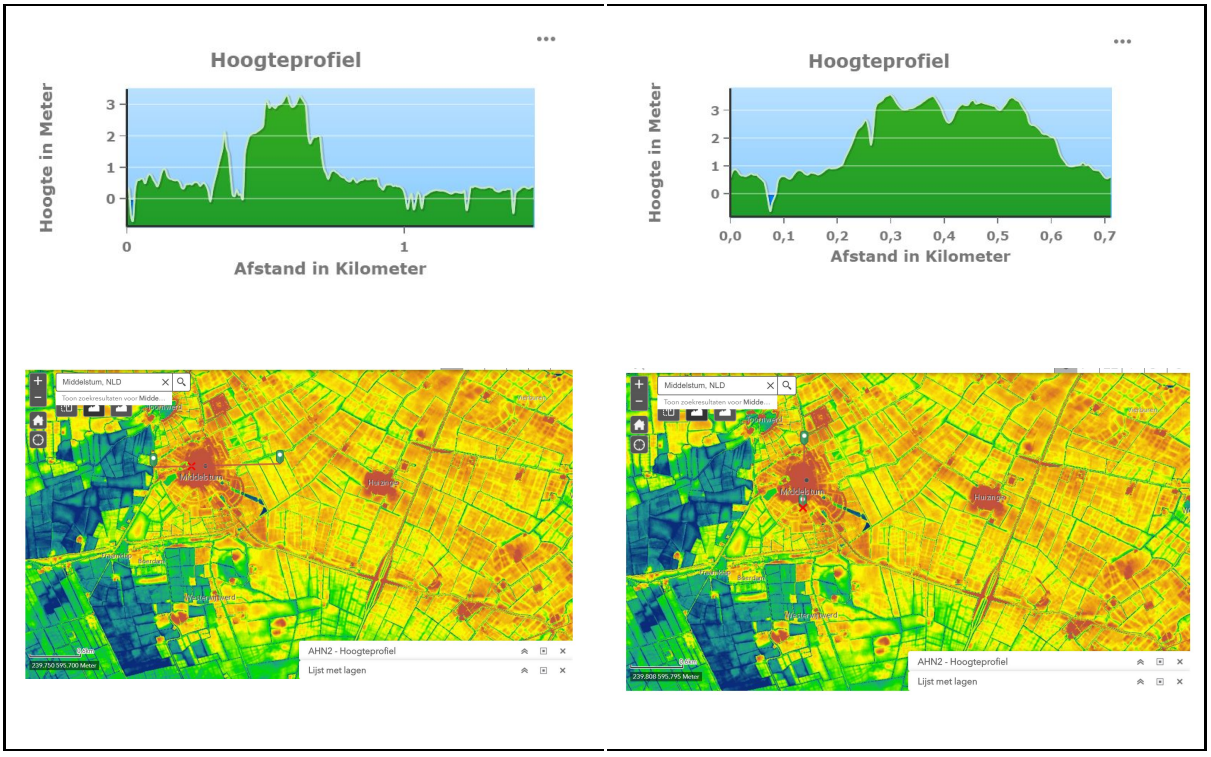

Figure 4.5.2 Height profiles and AHN images of Middelstum

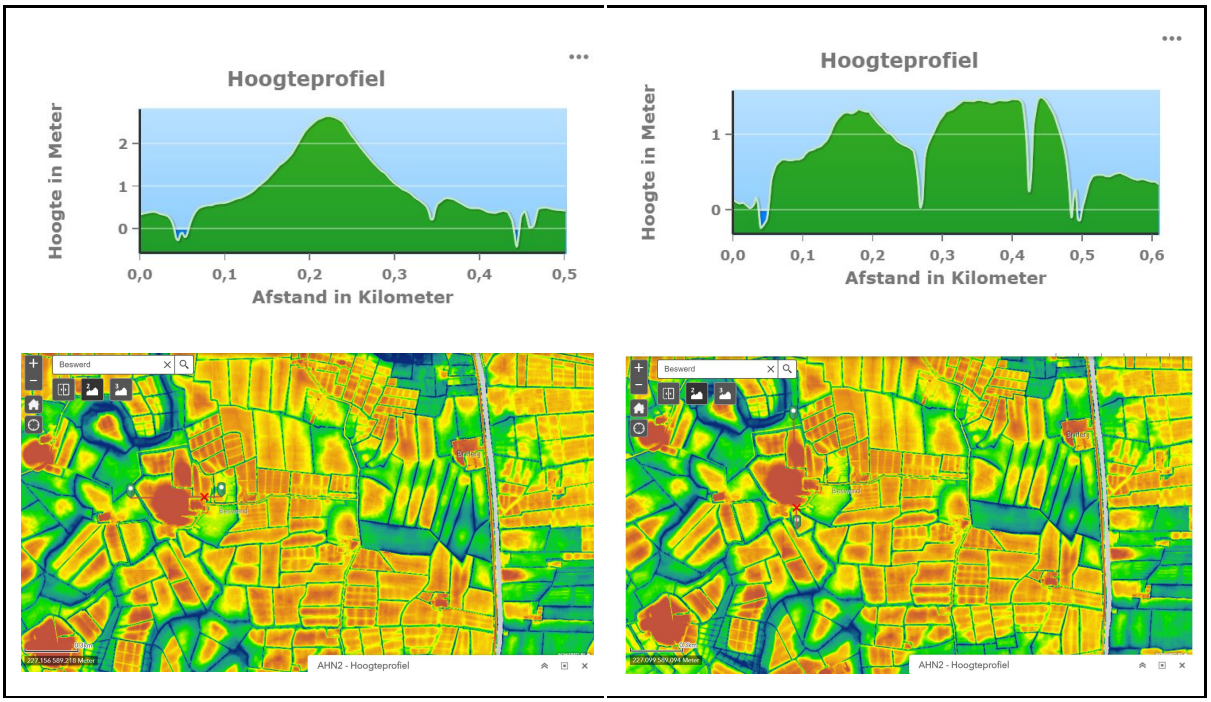

Figure 4.5.3 Height profiles and AHN images of Beswerd

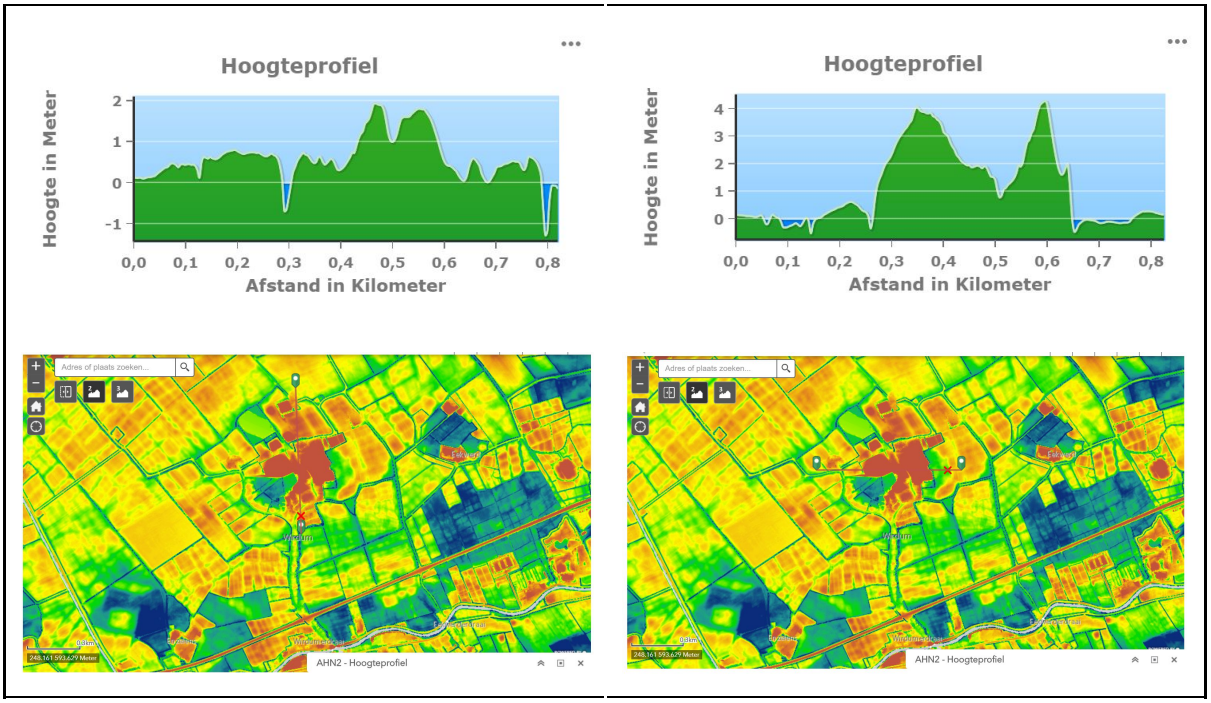

Figure 4.5.4 Height profiles and AHN images of Wirdum

4.6 3D visualisation of AHN data of terpen with QGIS

The shape of the terp has an influence on its liquefaction sensitivity. 3D models of the terp ground surface were made in QGIS with AHN2 data, see the figures 4.6.1 through 4.6.4. The methodology for downloading AHN data and creating a 3D model can be found in Appendix B3.

The Middelstum and Beswerd terp are stable in terms of their geometry. Especially, the Middelstum terp due to its radial structure. Furthermore, the Wirdum terp is less stable because the elevations change faster from high to low so the slopes are less shallow compared to the other two terpen.

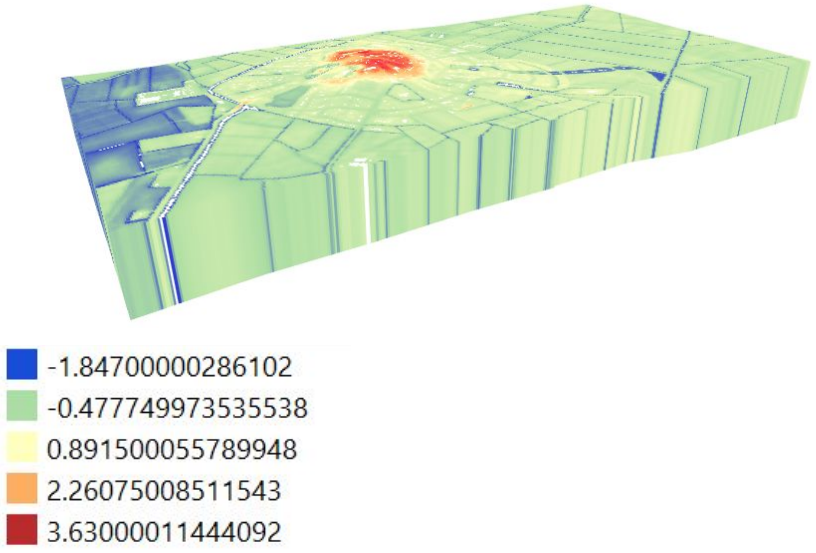

Figure 4.6.1 Middelstum in 3D with legend in metres

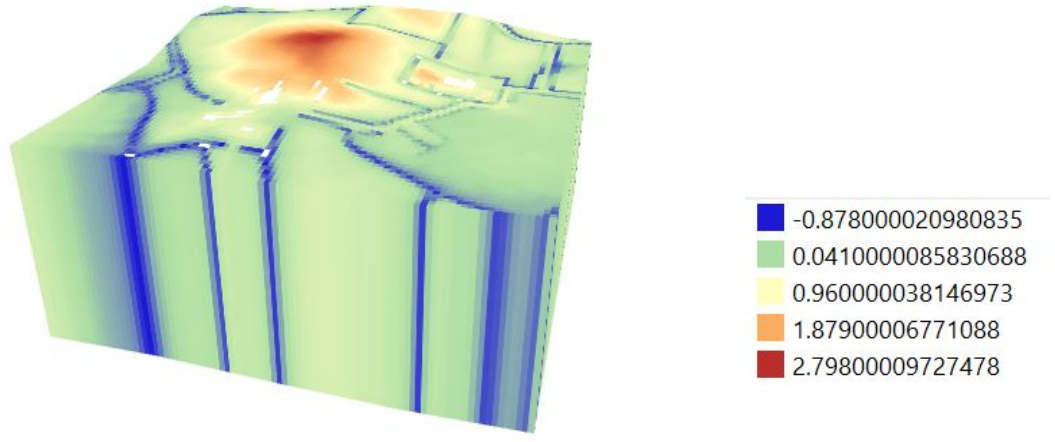

Figure 4.6.2 Beswerd in 3D with legend in metres

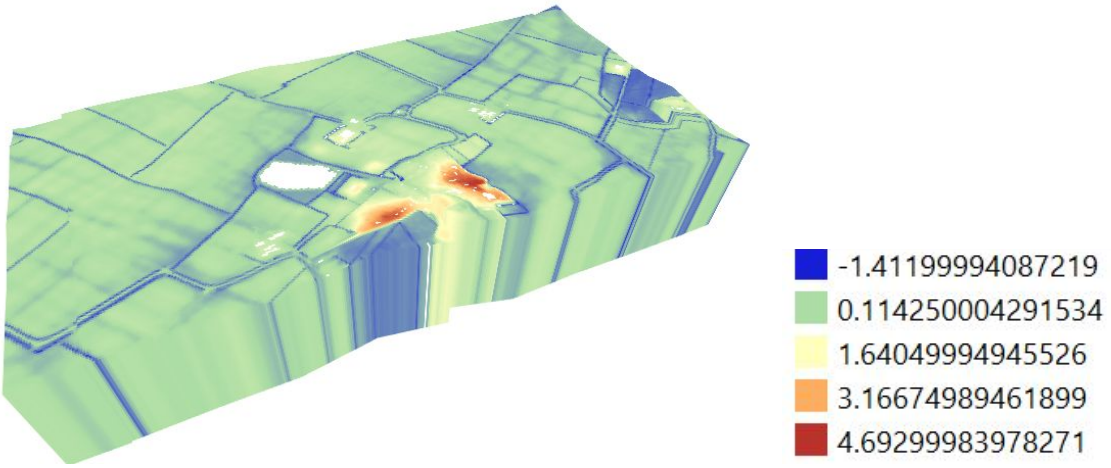

Figure 4.6.3 North of Wirdum in 3D with legend in metres

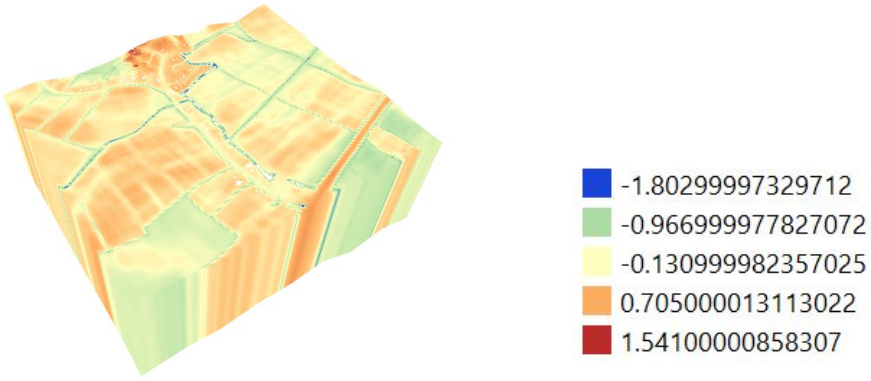

Figure 4.6.4 South of Wirdum in 3D with legend in metres

5. Methodology

Soil classification

In order to derive soil types from CPT data, the CPT data must be segmented in soil layers. The layers were defined with the use of the friction ratio and cone resistance values versus depth graphs. Afterwards the average friction ratio, sleeve friction and cone resistance for each layer were calculated with MATLAB. Then, the classification schemes presented in section 3.2 were applied to the data.

Soil unit weight

The volumetric weight of the soil must be known to estimate the vertical stress in order to calculate the soil behaviour index. Since the underground is made up of several soil types, each soil type has its own volumetric weight. The whole soil column was assumed to be saturated. The soil classes from the Robertson et al. (1986) soil classification chart were used. The specific soil classes from the NEN 6740 table were not identical to the classes of the Robertson soil classes. However with the use of the cone resistance, a good approximation could be made. The reasoning for each determination is provided in the results, section 6.

Soil behaviour index

The I_c values were determined as explained in section 3.3. The vertical stresses and effective vertical stresses were calculated as taught in the course: Soil Mechanics AESB2330 (2018/2019), assuming that the soil column was fully saturated. The calculations were done in MATLAB, the scripts can be found in Appendix C1. The goal is to determine the soil behaviour characteristics of the terpen in order to evaluate the liquefaction potential.

6. Results

Note that * stands for the average values.

Table 6.1 Soil classification Middelstum terp					
layer	**layer w.r.t. ground level (m)**	**q_c* (MPa)**	**R_f* (%)**	**soil type based on ATAR**	**soil type based on Robertson et al.**
1	0.0-1.5	0.35	7.6	peaty clay	2: organic material
2	1.5-9.3	1.08	3.1	clayey sand	5: clayey silt to silty clay
3	9.3-11.8	5.36	1.6	clayey sand	7: silty sand to sandy silt
4	11.8-13.0	5.46	2.9	firm clay	6: sandy silt to clayey silt
5	13.0-23.4	1.80	6.8	peat or peaty clay	3: clay

Table 6.2 Soil unit weight Middelstum terp					
	layer w.r.t. ground level (m)	**q_c*(MPa)**	**soil type based on Robertson et al.**	**soil type & reasoning**	**γ_{sat}(kN/m3)**
1	0.0-1.5	0.34	organic material	peat, moderately loaded - organic material - qc > 0.2	13
2	1.5-9.3	1.09	clayey silt to silty clay	loam & weak sandy - loam - qc =1	19
3	9.3-11.8	5.48	silty sand to sandy silt	sand weak silty, clayey - sand - qc=5	20
4	11.8-13.0	5.16	sandy silt to clayey silt	sand strong clayey and silty - sand - qc=5	21
5	13.0-23.4	1.80	clay	clean clay	17

Table 6.3 I_c calculation Middelstum terp						
	layer w.r.t. ground level (m)	**thickness (m)**	**midpoint layer w.r.t. ground level (m)**	**q_c* (MPa)**	**f_s* (MPa)**	**I_c***
1	0.0-1.5	1.5	1.5/2= 0.8	0.34	2.4e-2	4.7
2	1.5-9.3	7.8	1.5+7.8/2= 5.4	1.09	2.6e-2	3.8
3	9.3-11.8	2.5	1.5+7.8+2.5/2= 10.6	5.48	8.6e-2	3.4
4	11.8-13.0	1.2	1.5+7.8+2.5+1.2/2= 12.4	5.16	1.2e-1	3.3
5	13.0-23.4	10.4	1.5+7.8+2.5+1.2+10.4/2=18.2	1.80	1.2e-1	3.3

Table 6.4 Soil classification Beswerd terp					
layer	**layer w.r.t. ground level (m)**	**q_c* (MPa)**	**R_f* (%)**	**soil type based on ATAR**	**soil type based on Robertson et al.**
1	0.0-0.9	1.55	3.76	moderate clay	4: silty clay to clay
2	0.9-5.4	1.12	1.42	clayey sand	7: silty sand to sandy silt
3	5.4-6.3	4.24	0.51	silty sand	8: sand to silty sand
4	6.3-10.7	2.79	0.90	clayey sand	7: silty sand to sandy silt
5	10.7-15.0	5.23	0.70	sand	8: sand to silty sand
6	15.0-26.1	5.08	1.34	silty sand	7: silty sand to sandy silt
7	26.1-27.2	25.96	0.81	sand	9: sand
8	27-2-30.1	11.08	1.03	sand	9: sand

Table 6.5 Soil unit weight Beswerd terp					
	layer w.r.t. ground level (m)	**q_c* (MPa)**	**soil type based on Robertson et al.**	**soil type & reasoning**	**γ_{sat} (kN/m3)**
1	0.0-0.9	1.55	4: silty clay to clay	clay, weak sandy (moderate) - clay - qc close to 1.5 MPa	18
2	0.9-5.4	1.12	7: silty sand to sandy silt	loam, weak sandy (weak) - qc close to 1 MPa - silt and sand	19

3	5.4-6.3	4.24	8: sand to silty sand	sand weak silty, clayey - sand and silt - qc in 5-20 MPa range	20
4	6.3-10.7	2.79	7: silty sand to sandy silt	loam, weak sandy (weak) - qc close to 1 MPa - silt and sand	19
5	10.7-15.0	5.23	8: sand to silty sand	sand weak silty, clayey - sand and silt - qc in 5-20 MPa range	20
6	15.0-26.1	5.08	7: silty sand to sandy silt	loam, weak sandy (weak) - qc close to 1 MPa - silt and sand	19
7	26.1-27.2	25.96	9: sand	clean sand (solid) - sand - qc close to 25 MPa	22
8	27-2-30.1	11.08	9: sand	clean sand (moderate) - sand - qc close to 15 MPa	20

Table 6.6 I_c calculation Beswerd terp

	layer w.r.t. ground level (m)	**thickness (m)**	**midpoint depth w.r.t. ground level (m)**	**q_c* (MPa)**	**f_s* (MPa)**	**γ_{sat} (kN/m3)**	**I_c***
1	0.0-0.9	0.9	0.9/2= 0.5	1.55	5.8e-2	18	4.4
2	0.9-5.4	4.5	0.9+4.5/2= 3.2	1.12	1.3e-2	19	4.1
3	5.4-6.3	0.9	0.9+4.5+0.9/2 = 5.9	4.24	2.3e-2	20	3.9
4	6.3-10.7	4.4	0.9+4.5+0.9+4.4/2= 8.5	2.79	2.3e-2	19	3.9
5	10.7-15.0	4.3	0.9+4.5+0.9+4.4+4.3/2 = 12.9	5.23	3.8e-2	20	3.7
6	15.0-26.1	11.1	0.9+4.5+0.9+4.4+4.3+11.1/2= 20.6	5.08	6.1e-2	19	3.6
7	26.1-27.2	1.1	0.9+4.5+0.9+4.4+4.3+11.1+1.1/2= 26.7	25.96	2.2e-1	22	3.2
8	27-2-30.1	2.9	0.9+4.5+0.9+4.4+4.3+11.1+1.1+2.9/2= 28.7	11.08	1.1e-1	20	3.5

Table 6.7 Soil classification Wirdum terp					
layer	**layer w.r.t. ground level (m)**	**q_c* (MPa)**	**R_f* (%)**	**soil type based on ATAR**	**soil type based on Robertson et al.**
1	0.0-1.8	1.05	2.83	loam	5: clayey silt to silty clay
2	1.8-6.4	0.53	1.58	firm clay	1: sensitive fine grained
3	6.4-8.5	13.03	1.01	sand	9: sand
4	8.5-11.1	4.73	2.55	firm clay	6: sandy silt to clayey silt
5	11.1-18.5	17.90	1.71	clayey sand	8: sand to silty sand

6.8 Soil unit weight Wirdum terp					
	layer w.r.t. ground level (m)	**q_c* (MPa)**	**soil type based on Robertson et al.**	**soil type & reasoning**	**γ_{sat}(kN/m3)**
1	0.0-1.8	1.05	5: clayey silt to silty clay	loam weak sandy - qc close to 1 - clay and silt	19
2	1.8-6.4	0.53	1: sensitive fine grained	sensitive fine grained (Bagińska, 2016)	17.5
3	6.4-8.5	13.03	9: sand	clean moderate sand - qc close to 15 - sand	20
4	8.5-11.1	4.73	6: sandy silt to clayey silt	sand strong silty clayey - qc between 2 to 15 - sand, clay and silt	20
5	11.1-18.5	17.90	8: sand to silty sand	sand weak silty clayey - qc between 5 to 20 - sand and silt	21

Table 6.9 I_c calculation Wirdum terp							
	layer w.r.t. ground level (m)	**thickness (m)**	**midpoint layer w.r.t. ground level (m)**	**q_c* (MPa)**	**f_s* (MPa)**	**γ_{sat} (kN/m3)**	**I_c***
1	0.0-1.8	1.8	1.8/2 = 0.9	1.05	2.9e-2	19	4.2
2	1.8-6.4	4.6	1.8 + 4.6/2 = 4.1	0.53	8.5e-3	17.5	4.3
3	6.4-8.5	2.1	1.8+4.6+2.1/2= 7.5	13.03	1.3e-1	20	3.2
4	8.5-11.1	2.6	1.8+4.6+2.1+2.6/2= 9.8	4.73	8.5e-2	20	3.4
5	11.1-18.5	7.4	1.8+4.6+2.1+2.6+7.4/2= 14.8	17.90	2.6e-1	21	3.0

7. Discussion

As indicated in section 3.3, the combination of an n exponent of 1 and I_c lower than 2.6 indicates a liquefaction case. Hence, the results conclude that all the three terpen are not prone to liquefaction. Furthermore, other site effects can influence the liquefaction potential, such as construction, but these are out of the scope of this report.

The soil types were defined with the use of CPT data from DINOloket. Processes such as overconsolidation might have taken place. These could have had an effect on the graphs of the CPT data, by increasing or decreasing the sleeve friction, friction ratio and cone resistance values. As a consequence the determined soil classes can be slightly off. Another consequence is an over- or underestimation of the soil behaviour index.

Furthermore, the soil unit weights were based on the soil class and cone resistance. Here the soil classes did not coincide with the soil classes of NEN 6470. This might have lowered the accuracy. It would have been more reliable if the soil unit weight was directly derived from more appropriate CPT data that includes measured densities. Moreover, NEN 6740 was used, which is now outdated. Hence, it would have been better to have used NEN-EN 1997. Also, the rounding errors might have played a minor role in the MATLAB generated calculations.

Moreover, Wirdum is located on the border of two AHN2 datasets, this prevented the creation of a 3D model of Wirdum in its completeness. Now, there are two 3D models of the north and south of Wirdum. If it were possible to merge these datasets in QGIS it would solve the problem. A complete 3D model of Wirdum would better represent the terp.

8. Conclusion

The goal of this report is to evaluate the liquefaction potential on the terpen that can be triggered due to induced earthquakes. The terpen that are prone to liquefaction have a shallow subsurface that is composed of young fine sands. The formations that had the highest liquefaction potential were the Naaldwijk and Eem formation, mostly because of their age and soil composition. Since the Naaldwijk formation is younger and positioned more shallow than the Eem formation, it is the most liquefiable. The three terpen that were investigated turned out to be safe from liquefaction based on the soil behaviour index values.

9. References

Aardbevingen (Gr.). (n.d.). Nam.nl. Retrieved September 2019, from https://www.nam.nl/feiten-en-cijfers/aardbevingen.html#iframe=L2VtY

AlleCijfers (2016). AlleCijfers.nl. Retrieved October 2019, from https://allecijfers.nl/buurt/middelstum-loppersum/

Alle rijksmonumenten in Middelstum | Monumenten - Rijksmonumenten.nl. (n.d.). Rijksmonumenten.nl. Retrieved October 2019, from http://rijksmonumenten.nl/monumenten/alle-rijksmonumenten/middelstum/

Arjaans, J. Terpafgravingen in Friesland, Historisch-geografisch tijdschrift; Jaargang 8; nr. 2 (1990), p. 57.

ATAR Geotechniek. (2016). Geotechnisch rapport betreffende een project aan de Oude Gracht 8 te Veenhuizen (110871). Retrieved from https://www.gemeentenoordenveld.nl/ruimtelijkeplannen/NL.IMRO.1699.2016PB017-vg01/b_NL.IMRO.1699.2016PB017-vg01_bd4.pdf

Bagińska, I. (2016). Estimating and verifying soil unit weight determined on the basis of SCPTu tests. Annals of Warsaw University of Life Sciences – SGGW. Land Reclamation, 48(3), 233–242. https://doi.org/10.1515/sggw-2016-0018

beeldbank Nederland. (2015). luchtfoto | Middelstum, Loppersum, Nederland [Photo]. Retrieved from https://www.aerophotostock.com/media/20e4563a-9924-428c-95c0-1509b72520a8-middelstum-loppersum-nederland-9-aug-2015-middelstum-behoo

Berendsen, H.J.A. (2008). Landschappelijk Nederland. Van Gorcum, Assen**.** p 72,74

Bodemrichtlijn. (2019). Bodemrichtlijn.nl. Retrieved October 2019, from https://www.bodemrichtlijn.nl/Bibliotheek/bodembescherming/archeologie/archeologie-begrippenlijst

Bosch, J.H.A., Harting, R., Gunnink, J.L. (2014). Lithologische karakterisering van de ondiepe ondergrond van Noord-Nederland (Topsysteem hoofdgebied 5) TNO 2014-R10680

Bosch, J.H.A., Harting, R. & Gunnink, J.L., 2014. Lithologische karakterisering van de ondiepe ondergrond van Noord-Nederland (Topsysteem hoofdgebied 5). TNO report 2014-R10680. Geological Survey of the Netherlands (Utrecht What is liquefaction? (2019). Usgs.gov. Retrieved September 2019, from https://www.usgs.gov/faqs/what-liquefaction?qt-news_science_products=0#qt-news_science_products

Bosschaart, A.M.W. and Driessen,P.M.M. (1989). Terpen in de Nederbetuwe en de Tielerwaard, Hist.-geogr.t, vol.7 pag. 10-17

Bosschaart, A.M.W. and Driessen, P.M.M. (1989). Terpen in de Nederbetuwe en de Tielerwaard, Hist.-geogr.t, vol.7 pag. 10-17

Boulanger, R.W., & Idriss, I. M. (2007). "Evaluation of cyclic softening in silts and clays." J. Geotechnical and Geoenvironmental Eng., ASCE 133(6), 641–52.

Boulanger, R. & Idriss, I. (2014): CPT and SPT based liquefaction triggering procedures.– Rep No UCDCGM-14 1, University of California at Davis, Davis, CA

Cone Penetration Testing (CPT). (n.d.). Usgs.gov. Retrieved September 2019, from https://www.usgs.gov/natural-hazards/earthquake-hazards/science/cone-penetration-testing-cpt?qt-science_center_objects=0#qt-science_center_objects

Correction wording flood risks for the Netherlands in IPCC report (n.d.). PBL Netherlands Environmental Assesment Agency. (n.d.). Retrieved September 2019, from https://www.pbl.nl/en/dossiers/Climatechange/content/correction-wording-flood-risks

CPT 101: Determining Soil Profiles from CPT Data. (n.d.). Vertekcpt.com. Retrieved October 2019, from http://www.vertekcpt.com/blog/cpt-101-determining-soil-profiles-from-cpt-data#.XadpS-gzY2x

Delvigne, J. (2008). Middag Humsterland – op het spoor van een eeuwenoud wierdenlandschap. Archeologie in Groningen 4. 96p.

Doesburg J. van. and Stöver J., Terpen en wierden: verleden, heden en toekomst. (2018). Rijksdienst voor het Cultureel Erfgoed.

Wayne Clough, G., Jotaro Iwabuchi; Shafli Rad, N. & Kuppusamy, T. (1989). Influence of Cementation on Liquefaction of Sands. Journal of Geotechnical Engineering. Vol 115, No 8. https://doi.org/10.1061/(ASCE)0733-9410(1989)115:8(1102)
Gans, W. de. (2007). Quaternary. In: Wong Th.E., Batjes D. A. J., Jager J. de (eds). Geology of the Netherlands. KNAW, Amsterdam, 354 p.
Gillins, D.T. (2012). Mapping The Probability and Uncertainty of Liquefaction-Induced Ground Failure, PhD thesis University of Utah, 2012
Green, R. A., Bommer, J. J., Stafford, P. J., Maurer, B. W., Edwards, B., Kruiver, P. P.,Rodriguez-Marek, A., de Hicks, M.A. & Vardon, P.J. (2019). AESB2330 Soil Mechanics [course]
Lange, G., Oates, S. J., Storck, T., Omidi, P., Bourne, S. J., & van Elk, J., 2018. Liquefaction Hazard Pilot Study for the Groningen Region of the Netherlands due to Induced Seismicity, NAM
H. Tsuchida, (1970). ‘’Prediction and countermeasure against liquefaction in sand deposits,” in Proceedings of the Seminar of the Port and Harbour Research Institute, vol. 3, pp. 1–3, Ministry of Trans-port, Yokosuka, Japan.
Herwig, G. (1911). No. 42 Ferwerd- Het afgraven van een terp [Photo]. Retrieved from http://www.industriespoor.nl/Terpafgravingen.htm
Idriss, I.M. (1999) An update to the Seed-Idriss simplified procedure for evaluating liquefaction potential. Proc., TRB Workshop on New Approaches to Liquefaction, Publication No. FHWARD-99- 165, Federal Highway Administration.
Image from terpen exposition in Westerkwartier, in the church of Niehove. (n.d.). [Photo]. Retrieved from https://www.geographixs.com/g1h4sect1gevaar-van-water.html
Image of terpen of the Netherlands, Museon, Den Haag (n.d.) [Photo]. Retrieved from https://www.geographixs.com/g1h4sect1gevaar-van-water.html
Ishihara, K. (1985). Stability of natural deposits during earthquakes. Proceedings 11th International Conference on Soil Mechanics and Foundation Engineering, 1985, 321-376.
Ishihara, K. and Takatsu, H. (1978). Effects of overconsolidation and K0 conditions on the liquefaction characteristics of sands. Proceedings of the First Caribbean Conference on Earthquake Engineering, Port-ofSpain, Trinidad, 1978.
Kleber, A., Terhorst, B., Bullmann, H., Hülle, D., Leopold, M., & Müller, S. et al. (2013). Subdued Mountains of Central Europe. Developments In Sedimentology, 9-93. doi:10.1016/b978-0-444-53118-6.00002-7
KNMI - Aardbevingen door gaswinning. (n.d.). Knmi.nl. Retrieved September 2019, from https://www.knmi.nl/kennis-en-datacentrum/uitleg/aardbevingen-door-gaswinning
KNMI - Seismische hazardkaart. (2017). Nationaalcoordinatorgroningen.nl. Retrieved September 2019, from https://www.nationaalcoordinatorgroningen.nl/onderwerpen/knmi-seismische-hazardkaart
Korff, M. Lange, de. L., Meijers, P., Wiersma,A., Kloosterman, F. (2016). Liquefaction sensitivity of the shallow subsurface of Groningen. *NAM*.
Kruiver, P., de Lange, G., Wiersma, A., Meijers, P., Korff, M., Peeters, J., Stafleu, J., Harting,R., Dambrink, R., Busschers, F., Gunnink, J. (2015) Geological schematisation of the shallow subsurface of Groningen. Deltares.
Kwaliteit | DINOloket. (n.d.). Dinoloket.nl. Retrieved October 2019, from https://www.dinoloket.nl/kwaliteit
Lancaster, N., 2009, Aeolian features and processes, *in* Young, R., and Norby, L., Geological Monitoring: Boulder, Colorado, Geological Society of America, p. 1-25, doi: 10.1130/2009.
Leeuwardse courant. (1900). Hoogste terp in Friesland. *Leeuwardse courant*.
Lunne T, Robertson PK, Powell JJM (1997): Cone Penetration Testing in Geotechnical Practice. – Blackie Academic & Professional, London, 2
Maljers, D., Dubelaar, W, Stafleu, J., Busschers, F., Dambrink, R. and Schokker, J., 2016. Modelleerwerkwijze GeoTOP modelgebied Oostelijke Wadden en aandachtspunten GeoTOP versie 1.3, stand 11 maart 2016. TNO report 060.21052/01.06-1IV
Meijles, E. (2015). De ondergrond van Groningen: een geologische geschiedenis. *NAM*.
Mulder, M., & Perey, P. (2018). *Gas Production and Earthquakes in Groningen; Reflection on Economic and Social Consequences*. *Papers.ssrn.com*. Retrieved September 2019, from https://papers.ssrn.com/sol3/papers.cfm?abstract_id=3206278

Mulder E. Fj., Geluk M.C., Ritsema I.L., Westerhoff W.E. and Wong T.E. (2003). De ondergrond van Nederland. Wolters Noordhoff, Groningen, p 379.
Nagase H., Shimizu K., Hiro-oka A., Mochinaga S. and Ohta S. (2000) : Effects of over-consolidation on liquefaction strength of sandy soil samples, Proc. of the 12th WCEE, pp.1133.1-1133.8. Kruiver, P. P., Wiersma, A., Kloosterman, F. H., de Lange, G., Korff, M., Stafleu, J., Busschers, F. S., Harting, R., Gunnink, J. L., Green, R. A., van Elk, J., & Doornhof, D. (2017). Characterisation of the Groningen subsurface for seismic hazard and risk modelling. *Netherlands Journal of Geosciences*, *96*(5), s215–s233. https://doi.org/10.1017/njg.2017.11
NCG (2017). Kwartaalrapportage april-juni 2017. Groningen, Nationaal Coordinator Groningen.
NEN 6740 (n.d.). Joostdevree.nl. Retrieved October 2019, from http://www.joostdevree.nl/bouwkunde2/jpgw/wrijvingsgetal_3_qc_conusweerstand_nen_6740.jpg
Ngan-Tillard, D. J. M. (n.d.). Excavation of Jelsum terp [Photo].
Nicolay, J., Langen, de, G., Stöver, J., Aalbersberg, G., Bahlen, G., Bakker, M., ... Vos, P. C. (2019). De terp van Hogebeintum in boorkernen. In A. Nieuwhof, E. Knol, & J. Nicolay (Eds.), De hoogste terp van Friesland: Nieuw en oud onderzoek in Hogebeintum (Vol. 101, pp. 33-130). (Jaarverslagen van de Vereniging voor Terpenonderzoek; Vol. 101). Groningen: Vereniging voor Terpenonderzoek.
Normaal Amsterdams Peil (NAP) | Rijkswaterstaat. (2019). *Rijkswaterstaat.nl*. Retrieved September 2019, from https://www.rijkswaterstaat.nl/zakelijk/open-data/normaal-amsterdams-peil/index.aspx
Nuttle, W., & Portnoy, J. (1992). Effect of rising sea level on runoff and groundwater discharge to coastal ecosystems. Estuarine, Coastal And Shelf Science, 34(2), 203-212. doi:10.1016/s0272-7714(05)80106-4
Plaatsengids.nl. (2019). Plaatsengids.nl. Retrieved October 2019, from https://www.plaatsengids.nl/beswerd
R.A. Green, J.J. Bommer, P.J. Stafford, B.W. Maurer, B. Edwards, P.P. Kruiver, A. Rodriguez-Marek, G. de Lange, S.J. Oates, T. Storck, P. Omidi, S.J. Bourne, and J. van Elk (2018). Liquefaction Hazard Pilot Study for the Groningen Region of the Netherlands due to Induced Seismicity. NAM.
Rajapakse, R. (2016). Geotechnical engineering theoretical concepts. Geotechnical Engineering Calculations And Rules Of Thumb, 61-85. doi:10.1016/b978-0-12-804698-2.00005-2
RCE. (2007). *Wierde en/of borgterrein* [Photo]. Retrieved from https://nl.wikipedia.org/wiki/Lijst_van_rijksmonumenten_in_Loppersum_(gemeente)#/media/Bestand:Overzicht_-_Wirdum_-_20429883_-_RCE.jpg
Robertson, P., & Wride, C. (1997). CYCLIC LIQUEFACTION AND ITS EVALUATION BASED ON THE SPT AND CPT. National Center For Earthquake Engineering Research. p. 225-276
Robertson, P.K., 1990, Soil Classification Using CPT, Canadian Geotechnical Journal, Vol 27,No. 1, p. 151-158.
Robertson, P.K., Campanella, R.G., Gillespie, D. and Greig, J. (1986) Use of Piezometer Cone Data. Proceedings of American Society of Civil Engineers, ASCE, In-Situ 86 Specialty Conference, Blacksburg, 23-25 June 1986, 1263- 1280.
Robertson P.k,, 2012, Interpretation of in-situ tests – some insights.Mitchell Lecture-ISC'4 Brazil;
Schatkamers van het vroegmiddeleeuwse Friesland. (2015). *Historiek*. Retrieved September 2019, from https://historiek.net/schatkamers-van-het-vroegmiddeleeuwse-friesland/50303/
Schroor, M., (1998) Wonen op hoogten: het terpenlandschap van Middag-Humsterland' in: Landschappen van wereldformaat (themanummer Historisch-Geografisch Tijdschrift XVI (1998), 115
soil liquefaction (n.d.). Encyclopedia Britannica. Retrieved September, from https://www.britannica.com/science/soil-liquefaction
Terp Hegebeintum (n.d). Hegebeintum.info. Retrieved October 2019, from https://www.hegebeintum.info/historie
van Asch, Th. W. J., Malet, J. P., & van Beek, L. P. H. (2006). Influence of landslide geometry and kinematic deformation to describe the liquefaction of landslides: Some theoretical considerations. Engineering Geology, 88(1–2), 59–69. https://doi.org/10.1016/j.enggeo.2006.08.002
Vlek, C. (2019). Rise and reduction of induced earthquakes in the Groningen gas field, 1991–2018: statistical trends, social impacts, and policy change. *Environmental Earth Sciences*, *78*(3). doi:10.1007/s12665-019-8051-4

Vos, P.C., 2015. Origin of the Dutch coastal landscapes. PhD thesis, Utrecht University
Vos, PC. Bazelmans J. Weerts HJT & van der Meulen MJM (red). (2011). Atlas van Nederland in het Holoceen. Uitgeverij Bert Bakker. 94p
Whaley, J. (2009). The Groningen Gas Field. GEO ExPro. Retrieved September 2019, from https://www.geoexpro.com/articles/2009/04/the-groningen-gas-field
When Should You Consider SPT Testing Over CPT?. (2014). Vertekcpt.com. Retrieved November 2019, from http://www.vertekcpt.com/blog/spt-testing-vs-cpt-testing#.XcQg4FdKg2w
Wirdum (Groningen) | Plaatsengids.nl. (n.d.). *Plaatsengids.nl*. Retrieved October 2019, from https://www.plaatsengids.nl/wirdum-groningen
Woordenboek Encyclo. (n.d.). Encyclo.nl.Retrieved September 2019, from https://www.encyclo.nl/begrip/woordenboek
Youd, T.L., and Perkins, D.M. (1978). Mapping liquefaction-induced ground failure potential, Journal of the Geotechnical Engineering Division 104, No. GT4, 433-446.
Youd,T. L, Idriss, I. M., Ronald D. Andrus, Ignacio Arango; Gonzalo Castro; John T. Christian; Richardo Dobry; W. D. Liam Finn; Leslie F. Harder, Jr.; Mary Ellen Hynes; Kenji Ishihara; Joseph P. Koester; Sam S. C. Liao; William F. Marcuson, III; Geoffrey R. Martin; James K. Mitchell; Yoshiharu Moriwaki; Maurice S. Power; Peter K. Robertson; Raymond B. Seed; and Kenneth H. Stokoe, II (2001) Youd, T. L., Idriss, I. M., (2001) Liquefaction Resistance of Soils: Summary Report from the 1996 NCEER and 1998 NCEER/NSF Workshops on Evaluation of Liquefaction Resistance of Soils. Journal of Geotechnical and Geoenvironmental Engineering, 127(10): 817-833

10. Appendix

Appendix A1

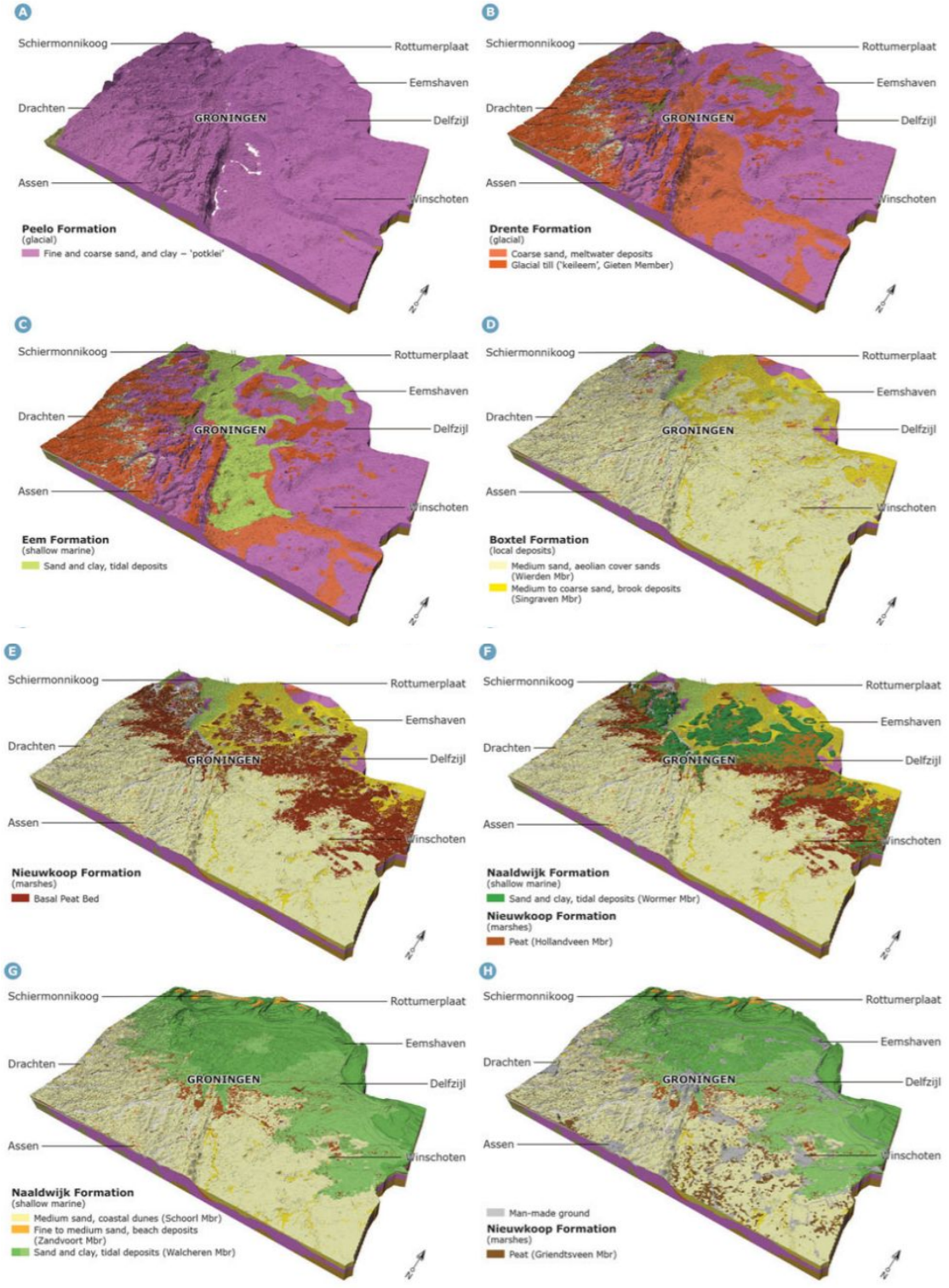

Figure A1.1 Overview of the formations made with Geotop (Kruiver et al, 2017)

Appendix A2

Table A2.1 NEN 6740 (NEN 6740, n.d.)

Type of soil		Representative mean value for the soil properties												
Name	Admixture	Consistency 1)	γ (kN/m3) 2)	γsat (kN/m3)	qc (Mpa) 3)6)	C´p	C´s	Cc	Ca 5)	Csw	Ey (Mpa) 6)	ϕ´(°)	c´(kPa)	f undr (kPa)
Gravel	weak silty	loose	17	18	15	500	-	0,008	0	0,003	75	32,5	-	-
		moderate	18	20	25	1000	-	0,004	0	0,002	125	35	-	-
		fixed/solid	19 or 20	20 or 21	30	1200 or 1400	-	0,003 or 0,002	0	0,001 or 0	150 or 200	37,5 or 40	-	-
	strong silty	loose	18	20	10	400	-	0,009	0	0,003	50	30	-	-
		moderate	19	21	15	600	-	0,006	0	0,002	75	32,5	-	-
		fixed/solid	20 or 21	22 or 22,5	25	100 or 1500	-	0,003 or 0,002	0	0,001 or 0	125 or 150	35 or 40	-	-
Sand	clean	loose	17	19	5	200	-	0,021	0	0,007	25	30	-	-
		moderate	18	20	15	600	-	0,006	0	0,003	75	32,5	-	-
		fixed/solid	19 or 20	21 or 22	25	1000 or 1500	-	0,003 or 0,002	0	0,001 or 0	125 or 150	35 or 40	-	-
	weak silty clayey		18 or 19	20 or 21	5 or 20	450 or 650	-	0,008 or 0,005	0	0,003 or 0,001	25 or 35	27 or 32,5	-	-
	strong silty clayey		18 or 19	20 or 21	2 or 15	200 or 400	-	0,019 or 0,009	0	0,006 or 0,001	20 or 30	25 or 30	-	-
Loam 4)	weak sandy	weak	-	19	1	25	650	0,168	0,004	0,056	2	27,5 or 30	0	50
		moderate	-	20	2	45	1300	0,084	0,002	0,028	5	27,5 or 32,5	2	100
		fixed/solid	-	21 or 22	3	70 or 100	1900 or 2500	0,049 or 0,030	0,001	0,017 or 0,005	10 or 20	27,5 or 35	5 or 7,5	200 or 300
	strong sandy		-	19 or 20	2	45 or 70	1300 or 2000	0,092 or 0,055	0,002	0,031 or 0,005	5 or 10	27,5 or 35	0 or 2	50 or 100
Clay	clean	weak	-	14	0,5	7	80	1,357	0,013	0,452	1	17,5	0	25
		moderate	-	17	1	15	160	0,362	0,006	0,121	2	17,5	10	50
		fixed/solid	-	19 or 20	2	25 or 30	320 or 500	0,168 or 0,126	0,004	0,056 or 0,042	4 or 10	17,5 or 25	25 or 30	100 or 200
	weak sandy	weak	-	15	0,7	10	110	0,759	0,009	0,253	1,5	22,5	0	40
		moderate	-	18	1,5	20	240	0,237	0,005	0,079	3	22,5	10	80
		fixed/solid	-	20 or 21	2,5	30 or 50	400 or 600	0,126 or 0,069	0,003	0,042 or 0,014	5 or 10	22,5 or 27,5	25 or 30	120 or 170
	strong sandy		-	18 or 20	1	25 or 140	320 or 1680	0,190 or 0,027	0,004	0,063 or 0,025	2 or 5	27,5 or 32,5	0 or 2	0 or 10
	organic	weak	-	13	0,2	7,5	30	1,69	0,015	0,55	0,5	15	0 or 2	10
		moderate	-	15 or 16	0,5	10 or 15	40 or 60	0,760 or 0,420	0,012	0,25 or 0,14	1 or 2	15	0 or 2	25 or 30
Peat	not preloaded	weak	-	10 or 12	0,1 or 0,2	5 or 7,5	20 or 30	7,59 or 1,81	0,023	2,530 or 0,6	0,2 or 0,5	15	2 or 5	10 or 20
	moderate loaded	moderate	-	12 or 13	0,2	7,5 or 10	30 or 40	1,81 or 0,900	0,016	0,6 or 0,3	0,5 or 1	15	5 or 10	20 or 30
Variation coeficient			0,05		-	0,25						0,1	0,2	

Appendix B1

Figure B1.1 Location of CPT (triangle) and borehole (circle) of Middelstum made in DINOloket
Note, the borehole is the left circle in the purple ring

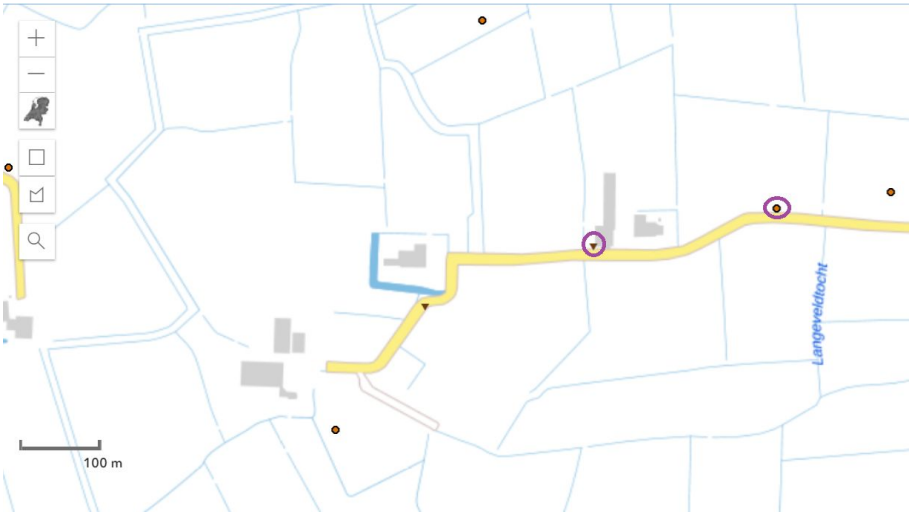

Figure B1.2 Location of CPT (triangle) and borehole (circle) of Beswerd made in DINOloket

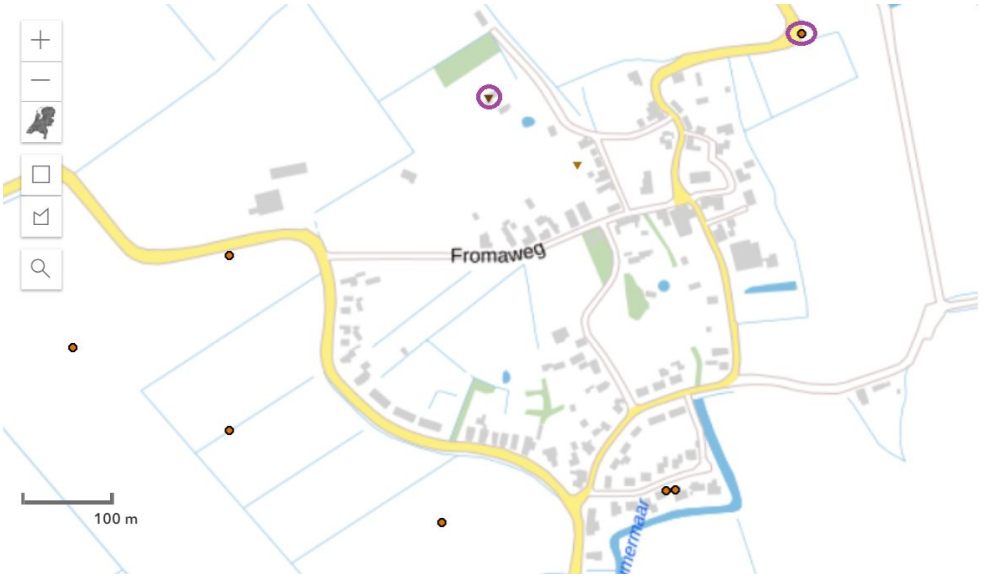

Figure B1.3 Location of CPT (triangle) and borehole (circle) of Wirdum made in DINOloket

Appendix B2

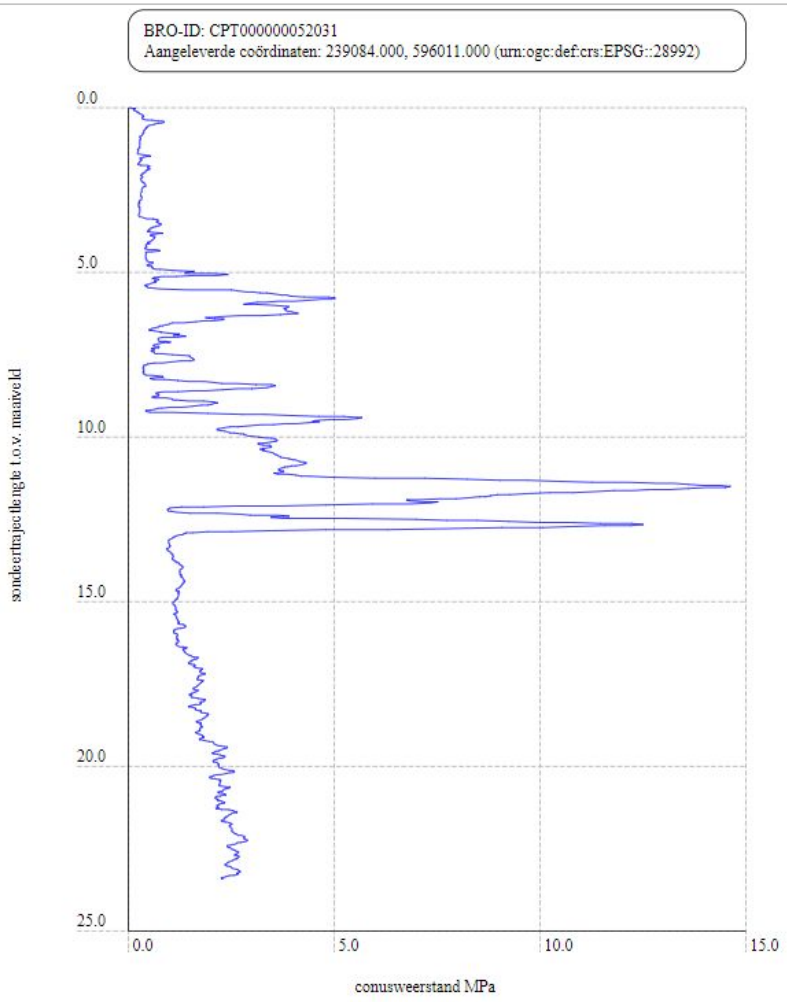

Figure B2.1 Middelstum cone resistance graph from DINOloket

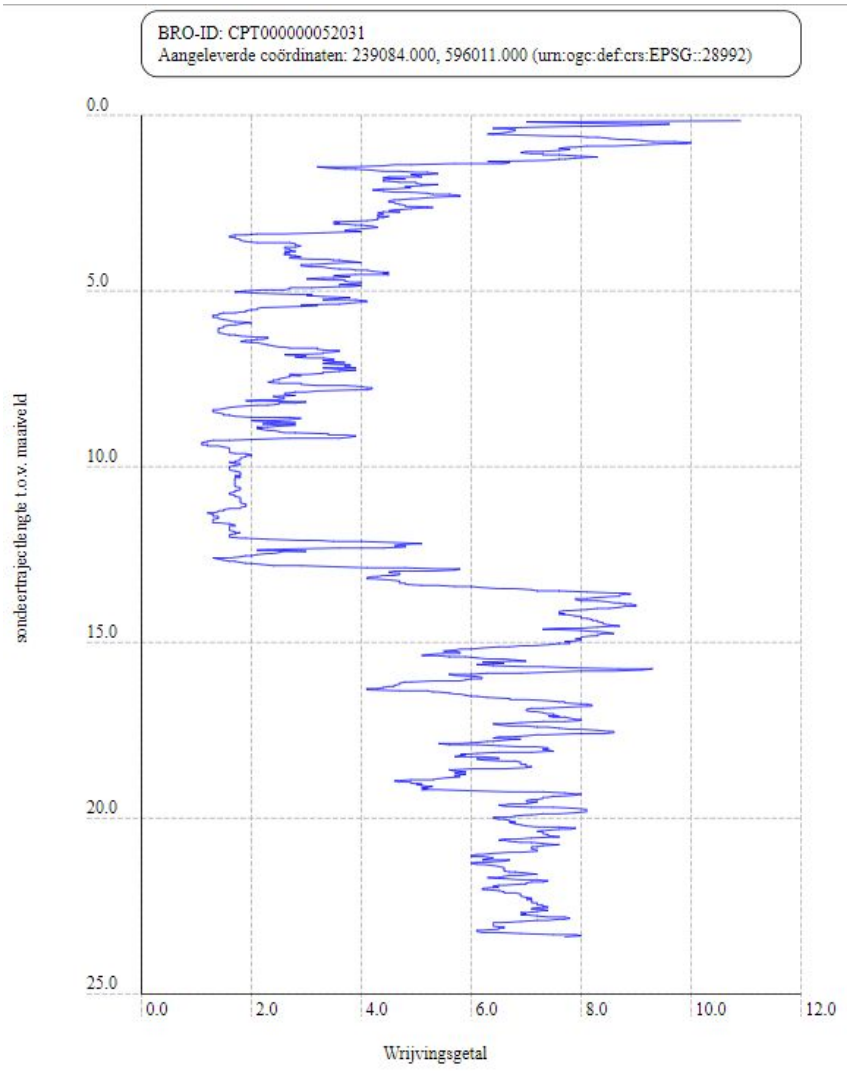

Figure B2.2 Middelstum friction ratio graph from DINOloket

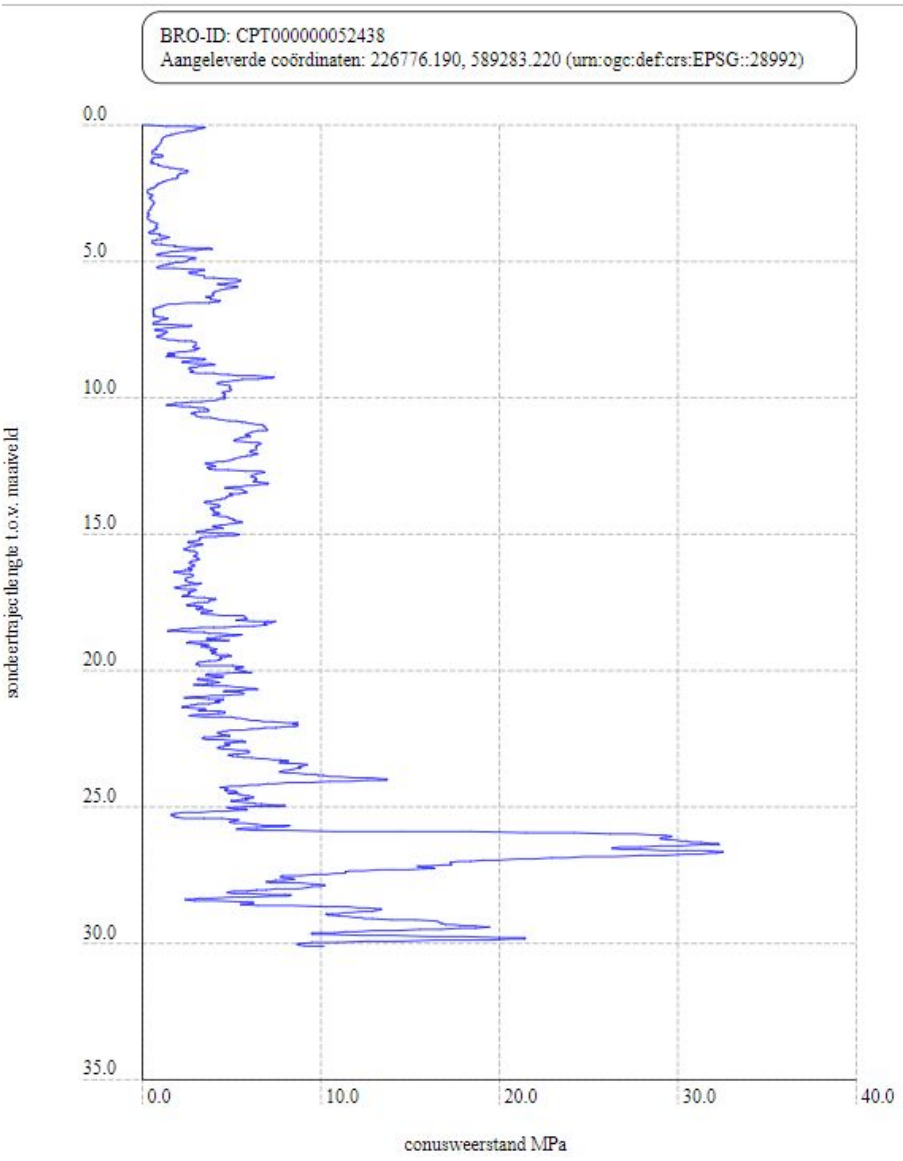

Figure B2.3 Beswerd cone resistance graph from DINOloket

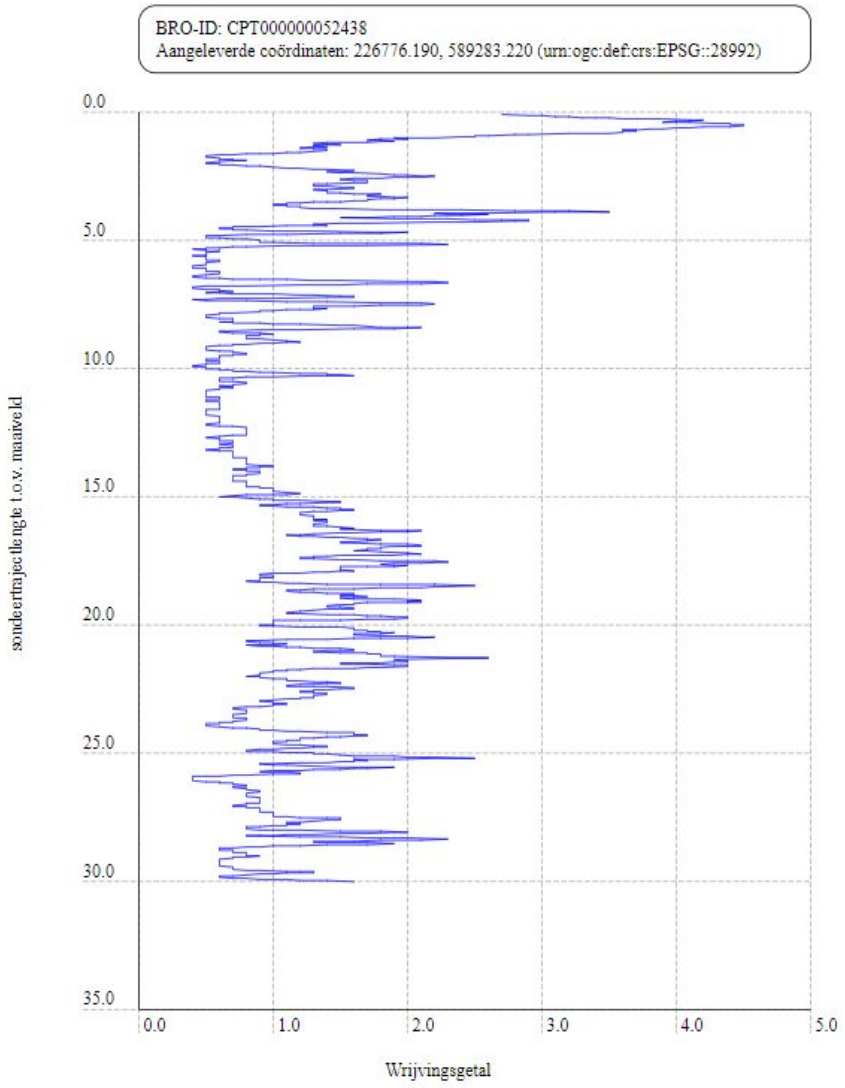

Figure B2.4 Besword friction ratio graph from DINOloket

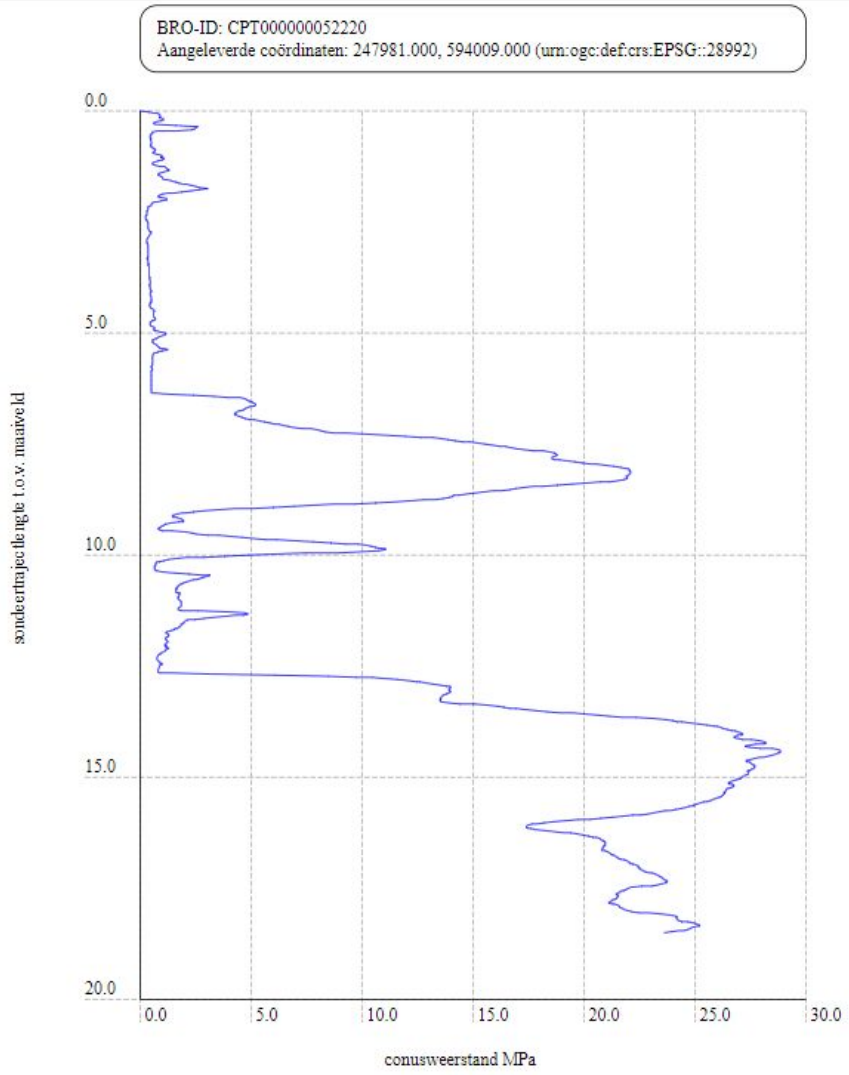

Figure B2.5 Wirdum cone resistance graph from DINOloket

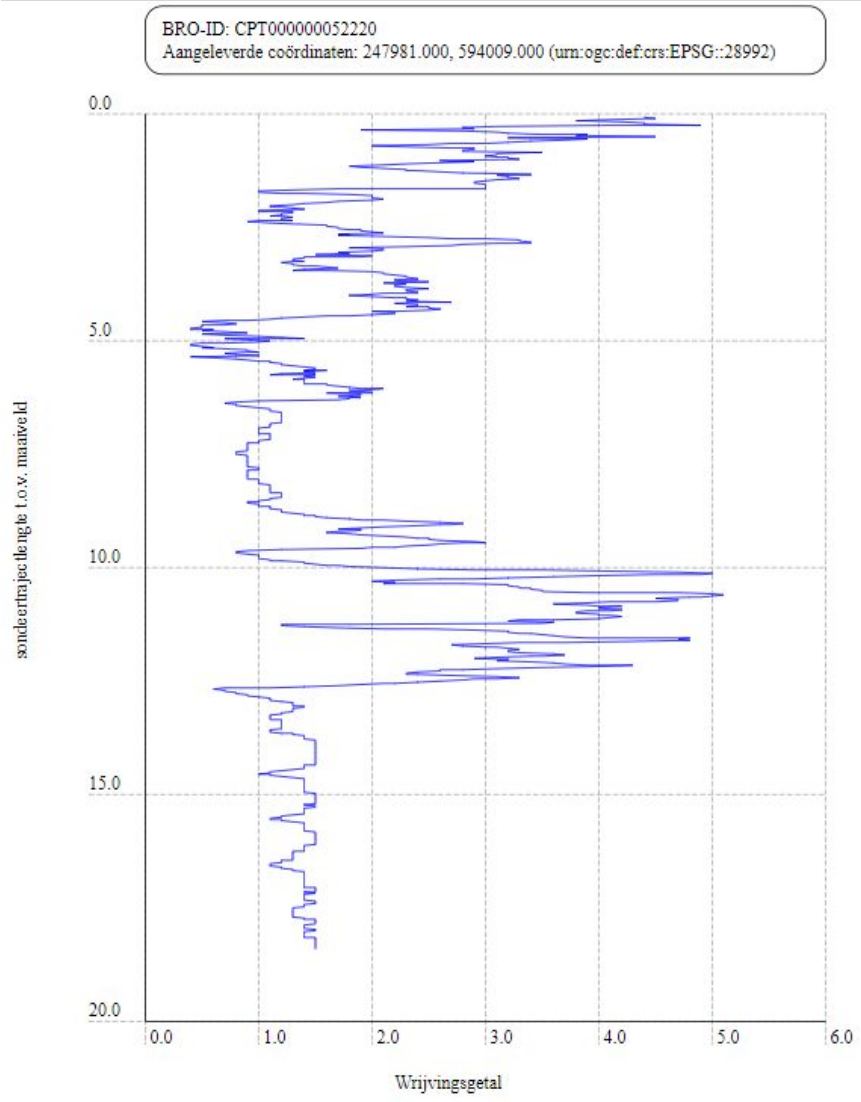

Figure B2.6 Wirdum friction ratio graph from DINOloket

Appendix B3

Methodology of 3D model creation

First the right AHN dataset had to be downloaded. The AHN datasets have a unique code that coincide with a certain section of the Netherlands, such as '07az2'. On pdokviewer.pdok.nl the right box could be found into which the terp was located. Then on pdok.nl the right AHN2 dataset could be downloaded, Datasets → AHN2 → AHN2 5 meter maaiveld raster, this was the maaiveld raster 5 metres option. This opened an XML file into which the code had to be found and its link. The link gave way to a zip file that contained a tif file. Afterwards, the Tif file could be added into QGIS as a new raster layer. In order to zoom into the terp and get a 3D model of only the terp the option raster > extractie > clipper > Bereik in kaartvenster selecteren, was used. Then the option Nieuwe 3D kaartweergave then in the new window in the settings change to elevation and add the raster layer and with the mouse the 3D model can be moved in all directions. Moreover, the vertical scale was set to 30 and 5 pixels were chosen for Wirdum and Beswerd. For Middelstum the vertical scale was changed to 20.

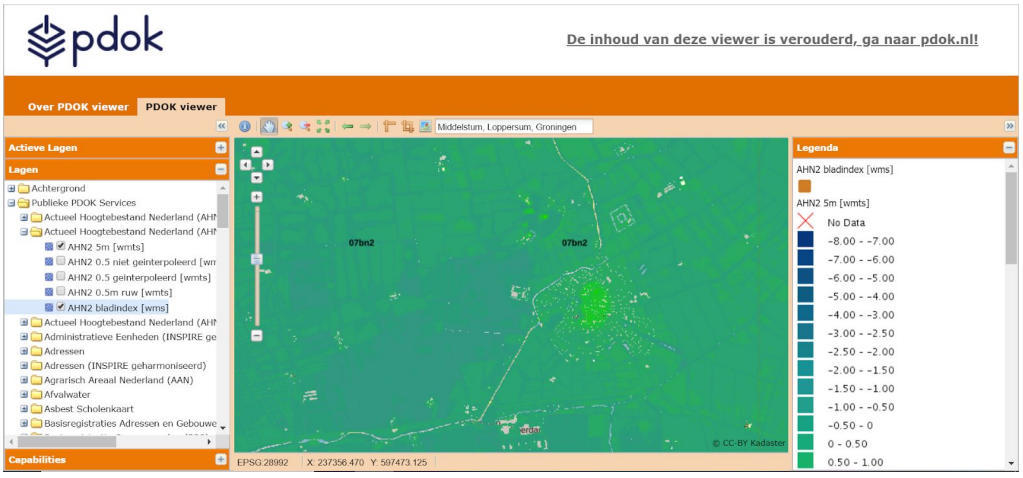

Appendix C1

```
% MATLAB script for Middelstum terp,for the last layer
Pa = 10e3; %Pa , reference stress
gw=10e3; %volumetric weight of water N/m3
qc= 1.80; %cone resistance
fs= 1.24e-1; %sleeve friction
zw = 18.2; %water height
svc= 1.5*13e3+7.8*19e3+2.5*20e3+1.2*21e3+(10.4/2)*17e3;
svc1=(svc)-(gw*zw); %effective stress
F1 = fs/(qc-svc);
F = -F1*100; %make it positive
n = 1;
Q1 = (qc-svc)/Pa;
Q2 = (Pa/svc1).^n;
Q = -Q1./Q2; %make it positive
AA1= 3.47-(log10(Q));
AA = AA1*AA1;
B1 =(1.22+log10(F));
B = B1*B1;
Ic= sqrt(AA+B)
```

```
%MATLAB script for Beswerd terp,for the last layer
Pa = 10e3; %Pa , reference stress
gw=10e3; %volumetric weight of water N/m3
qc= 11.08; %cone resistance
fs= 1.1e-1; %sleeve friction
zw = 28.7; %water height
svc=0.9*18e3+4.5*19e3+0.9*20e3+4.4*19e3+(4.3)*20e3+(11.1)*19e3+(1.1)*22e3+(2.9/2)*2
0e3;
svc1=(svc)-(gw*zw); %effective stress
F1 = fs/(qc-svc);
F = -F1*100; %make it positive
n = 1;
Q1 = (qc-svc)/Pa;
Q2 = (Pa/svc1).^n;
Q = -Q1./Q2; %make it positive
AA1= 3.47-(log10(Q));
AA = AA1*AA1;
B1 =(1.22+log10(F));
B = B1*B1;
Ic= sqrt(AA+B)
```

```
%MATLAB script for Wirdum terp,for the last layer
Pa = 10e3; %Pa , reference stress
gw=10e3; %volumetric weight of water N/m3
zw = 14.8; %water height
svc= 1.8*19e3+4.6*17.5e3+2.1*20e3+2.6*20e3+7.4/2*21e3;

qc= 17.9; %cone resistance
```

```
fs= 2.6e-1; %sleeve friction
svc1=(svc)-(gw*zw); %effective stress
F1 = fs/(qc-svc);
F = -F1*100; %make it positive
n = 1;
Q1 = (qc-svc)/Pa;
Q2 = (Pa/svc1).^n;
Q = -Q1./Q2; %make it positive
AA1= 3.47-(log10(Q));
AA = AA1*AA1;
B1 =(1.22+log10(F));
B = B1*B1;
Ic= sqrt(AA+B)
```